

1969

# A hybrid computer method for two dimensional calculations involving the Laplacian operator

Richard Lee Jaworski  
*Iowa State University*

Follow this and additional works at: <https://lib.dr.iastate.edu/rtd>

 Part of the [Engineering Commons](#)

## Recommended Citation

Jaworski, Richard Lee, "A hybrid computer method for two dimensional calculations involving the Laplacian operator " (1969).  
*Retrospective Theses and Dissertations*. 3748.  
<https://lib.dr.iastate.edu/rtd/3748>

This Dissertation is brought to you for free and open access by the Iowa State University Capstones, Theses and Dissertations at Iowa State University Digital Repository. It has been accepted for inclusion in Retrospective Theses and Dissertations by an authorized administrator of Iowa State University Digital Repository. For more information, please contact [digirep@iastate.edu](mailto:digirep@iastate.edu).

**This dissertation has been  
microfilmed exactly as received**

**70-7708**

**JAWORSKI, Richard Lee, 1942-  
A HYBRID COMPUTER METHOD FOR TWO  
DIMENSIONAL CALCULATIONS  
INVOLVING THE LAPLACIAN OPERATOR.**

**Iowa State University, Ph.D., 1969  
Engineering, general**

**University Microfilms, Inc., Ann Arbor, Michigan**

A HYBRID COMPUTER METHOD FOR TWO DIMENSIONAL  
CALCULATIONS INVOLVING THE LAPLACIAN OPERATOR

by

Richard Lee Jaworski

A Dissertation Submitted to the  
Graduate Faculty in Partial Fulfillment of  
The Requirements for the Degree of  
DOCTOR OF PHILOSOPHY

Major Subject: Nuclear Engineering

Approved:

Signature was redacted for privacy.

In Charge of Major Work

Signature was redacted for privacy.

Head of Major Department

Signature was redacted for privacy.

Dean of Graduate College

Iowa State University  
Ames, Iowa

1969

## TABLE OF CONTENTS

	Page
I. INTRODUCTION	1
II. THEORY	5
III. APPLICATION TO A NUCLEAR REACTOR	18
IV. PRESENTATION OF A HYBRID COMPUTER METHOD FOR SOLVING MULTIDIMENSIONAL DIFFUSION PROBLEMS	32
V. DIGITAL COMPUTER SOLUTION OF THE TWO DIMENSIONAL DIFFUSION PROBLEM	38
VI. RESULTS OF THE DIGITAL SOLUTION	44
VII. SUMMARY AND CONCLUSIONS	55
VIII. SUGGESTIONS FOR FURTHER STUDY	56
IX. LITERATURE CITED	58
X. ACKNOWLEDGMENTS	60
XI. APPENDIX A - THE CONTINUOUS SPACE, DISCRETE TIME METHOD APPLIED TO PARABOLIC DIFFUSION EQUATIONS	61
XII. APPENDIX B - THE PARALLEL MODAL METHOD APPLIED TO THE PARABOLIC DIFFUSION EQUATION	64
XIII. APPENDIX C - THE MIXED MODAL-SERIAL METHOD APPLIED TO THE PARABOLIC DIFFUSION EQUATION	66

## I. INTRODUCTION

Many natural phenomena are described by second order partial differential equations of several independent variables. Methods available for reducing the number of such variables are not always applicable, and the problem must be considered in terms of several dimensions. The electronic analog computer or differential analyzer with its ability to solve differential equations has long been used to consider these phenomena. The chief advantage of an analog computer is that one variable can be represented as continuous. In problems of more than one variable, a choice is made regarding which variable will be continuous and which variables can be practically considered in discrete form. For reasons of stability given by MacKay (12), the classical analog computer approach to multi-dimensional problems has been to discretize the space variables and represent the time variable as continuous. This is known as the method of discrete space, continuous time, DSCT. In this method, finite difference approximations are made for derivative terms involving the space variables. In problems involving first order time derivatives, if the space variable  $x$  is divided into  $N$  subspaces, the result of the difference approximations for the space derivative is a system of  $N$  simultaneous first order differential equations in which time is continuous. The chief disadvantage of this approach is that the accuracy and the amount of analog equipment required increases in proportion to the number of space points. Large analog computer systems of sizes ranging up to the 1500 amplifier Saturn computer in Great Britain have been built to handle systems of a large number of simultaneous equations with a high degree of accuracy. Examples

of this method are found in many analog references (9, 10, 15). In several cases, this method has been applied to two and three dimensional discrete space geometries. Illustrations of this multidimensional procedure are given by Howe and Haneman (8) and Bona (1).

In contrast to the discrete space, continuous time approach to partial differential equations is the method of continuous space, discrete time, CSDT, also known as the serial method. In this method the time derivatives are represented by difference expansions, and the space variable is related to the continuous analog machine time. If the range of the time variable is divided into  $K$  finite intervals or steps, the difference approximation for the time derivatives reduces the problem to a single differential equation of an order equal to the order of the space derivative. Therefore, only one group of analog elements is required for each time step, and the equipment requirements do not grow with the complexity of the problem. While this method easily accounts for moving boundaries and non-linear coefficients, it requires that the solution to the  $k - 1$  time step be available as input to the solution of the  $k^{\text{th}}$  time step, meaning a memory to play back this previous solution is necessary. This method sometimes requires that the solution for the  $k^{\text{th}}$  time step be found by an iteration process once the  $k - 1$  step solution is available. These two requirements prescribe that a hybrid computer be used for this method. Vichnevetsky (16) discusses the current hybrid technique for applying the serial method to the parabolic diffusion equation. This technique is shown in Appendix A. Various methods of solving the continuous space discrete time problem have been proposed by Calza-Bini (3), Witsenhausen (18), and Vichnevetsky (17). All of these deal with a one dimensional

space problem due to the fact that there is only one continuous variable on the analog computer. A third method used for solution of space and time dependent partial differential equations is the parallel-modal method. In this method the dependent variable is represented by a truncated series of  $N$  eigenmodes. The space dependent functions are the modes of the Helmholtz equation, and the time dependent coefficients of the eigenfunctions are solutions of ordinary differential equations which are found using the orthogonality property of the Helmholtz modes. Application of this method to a nuclear reactor is outlined in Appendix B. With this method, multi-dimensional space, time dependent solutions are possible when considering linear problems and simple geometries where a small number of modes are required for solution without truncation error. This method, first introduced by Carstairs and Taylor (4, 5), has been used by Caliguiri, et al. (2), and d'Hoop (6).

In order to apply the continuous space, discrete time method to problems in more than one space dimension, all partial derivatives, except the derivative of the continuous variable, are approximated by their Helmholtz eigenmodes. This method, described in Appendix C, is known as the mixed modal, serial method. Godts (7) applied this method to a nuclear reactor to describe the flux variation resulting from the ejection of a control rod from the Yankee reactor. Adding eigenmodes to represent space dimensions complicates the continuous space, discrete time method of solution for the dependent variable because instead of solving just one equation with this method, it is necessary to solve an equation for each mode used in the modal expansion.

Finite difference approximations to the partial derivatives eliminated using eigenmodes have been considered but discredited for hybrid computation using continuous space, discrete time because the approximation results in a set of differential equations, one equation for each increment of the approximated coordinate, rather than a single equation.

This study proposes a method for determining the multidimensional space dependence in terms of a single variable so that difference approximations for derivatives do not introduce more equations. Basically the approach is to relate the independent space variables to one variable so that a spatial geometry is described in one dimension. The method proposed in this study will be applied to the Laplacian operator because the Laplacian is multidimensional and frequently arises in boundary value problems solved by the hybrid computer. Because a hybrid computer was not available, a digital computer code was written to test the method when applied to a two-dimensional diffusion equation describing a nuclear reactor.

## II. THEORY

In this section, the basic principles of functions of several variables and functions of related variables are introduced. An illustration is given of the application of related variables to the evaluation of an analytical expression and to the development of the multidimensional Laplacian operator expressed in terms of one parametric variable. The operator in reduced variable representation is derived in two forms, one for application of this technique to a hybrid computer and another form for application to a digital computer.

The graph of a function of one variable,  $F(x)$ , is a curve whose independent and dependent variables constitute a two-dimensional coordinate system. The curve expresses the relationship between the independent and dependent variables. For a single valued function, specifying either variable immediately fixes the value of the other. Likewise the graph of a function of two independent variables,  $F(x,y)$ , is a surface described by a three-dimensional coordinate system. There are instances when it is convenient to express one of the independent variables in terms of another. That is,

$$F(x,y) = F(x,f(x))$$

where  $f(x)$  is a function selected to relate best the independent variables for the geometry and range of variables under consideration. This relationship between independent variables is often expressed by means of an intermediary variable called a parameter or parametric variable. The functions relating the parameter and the original independent variables are known as parametric equations. For example, substitution of the parametric equation

$$x_k = f_k(S)$$

of parameter  $S$  into the function  $\psi(x_1, x_2, \dots, x_k, \dots, x_k)$  gives

$$\psi(x_1, x_2, \dots, x_k, \dots, x_k) = \psi(f_1(S), f_2(S), \dots, f_k(S)).$$

It is important to note that a relationship between independent variables does not reduce the number of variables that must be considered in the formulation of the solution for the dependent variable. However a relationship between independent variables does reduce the number of such variables needed to describe the dependent variable once the solution has been determined. When using computational methods in which it is not possible to account for the values of several independent variables, this reduction is worthwhile. One sweep through the range of the parametric or the reduced variable can account for values from the entire range of the  $K$  independent variables. A given analytical expression of several dimensions can readily be evaluated along the path described by a single variable.

For example, given the D'Alembert solution of the wave equation (19) describing the motion of an infinite string with an initial displacement

$\phi(x)$ , where  $\phi(x) = \frac{1}{1 + 8x^2}$  and released from rest as

$$y(x,t) = \frac{1}{2} \left[ \frac{1}{1 + 8(x - at)^2} + \frac{1}{1 + 8(x + at)^2} \right].$$

The space variable  $x$  and the time variable  $t$  can be related so that

$$t = f(x) = \frac{t_{\max}}{2} \sin kx + \frac{t_{\max}}{2}$$

where  $t_{\max}$  is the maximum considered value of the time variable and  $k$  is a constant which determines the length of the  $x$  interval for each cycle of the time variable. When  $t$  is eliminated from  $y(x,t)$  the result is

$$y(x, f(x)) = \frac{1}{2} \left\{ \frac{1}{1 + 8 \left[ x - \frac{at}{\max} (\sin kx + 1) \right]^2} + \frac{1}{1 + 8 \left[ x + \frac{at}{\max} (\sin kx + 1) \right]^2} \right\}$$

$y(x, t)$  in this form can be evaluated over the range of both  $x$  and  $t$  by one sweep through the  $x$  variable.

The technique of relating variables can also be applied to solving multidimensional equations. Solutions to such equations are usually too complicated to be expressed analytically, and numerical methods involving integration over differential areas are used to develop finite difference equations which lead to a solution (14).

In the solution of differential equations whose independent variables are to be related, the function  $\psi(x_1, x_2, \dots, x_K)$  is first considered. Then multidimensional numerical methods are applied, except that the differential areas are modified so they can be described by the related independent variables. The resulting equations resemble those derived using standard multidimensional methods, and the number of independent variables needed in the calculation of the dependent variable has been reduced.

The application of the related independent variables technique to the Laplacian operator will now be considered. The first step in this development is to select a relationship between variables which meets the following requirements:

1. Describes the geometry of the coordinate system
2. Covers the range of independent variables continuously
3. Is adaptable to numerical methods.

Each coordinate system, Cartesian, cylindrical, or spherical, has a relationship between independent variables that would be appropriate for a specific problem. No set of relationships is general enough to describe all systems, yet the procedures used are similar. For the purposes of demonstration the  $r - \theta$  coordinate system will be used here. For the  $r - \theta$  system, the requirements are met by the spiral of Archimedes which is described by the parametric functions

$$\begin{aligned} r &= k_1 S \\ \theta &= k_2 S \end{aligned} \tag{1}$$

where  $k_1$  is the radial velocity of a point on the spiral per unit of the parametric variable  $S$ , and  $k_2$  is the angular velocity of the point on the spiral about the origin per unit of the parametric variable. This spiral is shown in Figure 1. Increasing  $k_2$  relative to  $k_1$  increases the number of revolutions the spiral completes per unit of  $r$  traversed. Elimination of  $S$  from the Equations 1 gives

$$r = \frac{k_1}{k_2} \theta . \tag{2}$$

The second step is to define a differential area. The boundaries of this area should be suggested by the locus described by the related independent variables. Common to both digital and hybrid applications of the derivation is the balance of leakage, removal, and production over this differential area. For the digital computer, many stationary discrete areas are coupled as members of a set of simultaneous equations. In the hybrid solution, one differential area is repeatedly moved over the geometry along the locus described by the related independent variables. This single area is coupled to values of the dependent variable calculated for

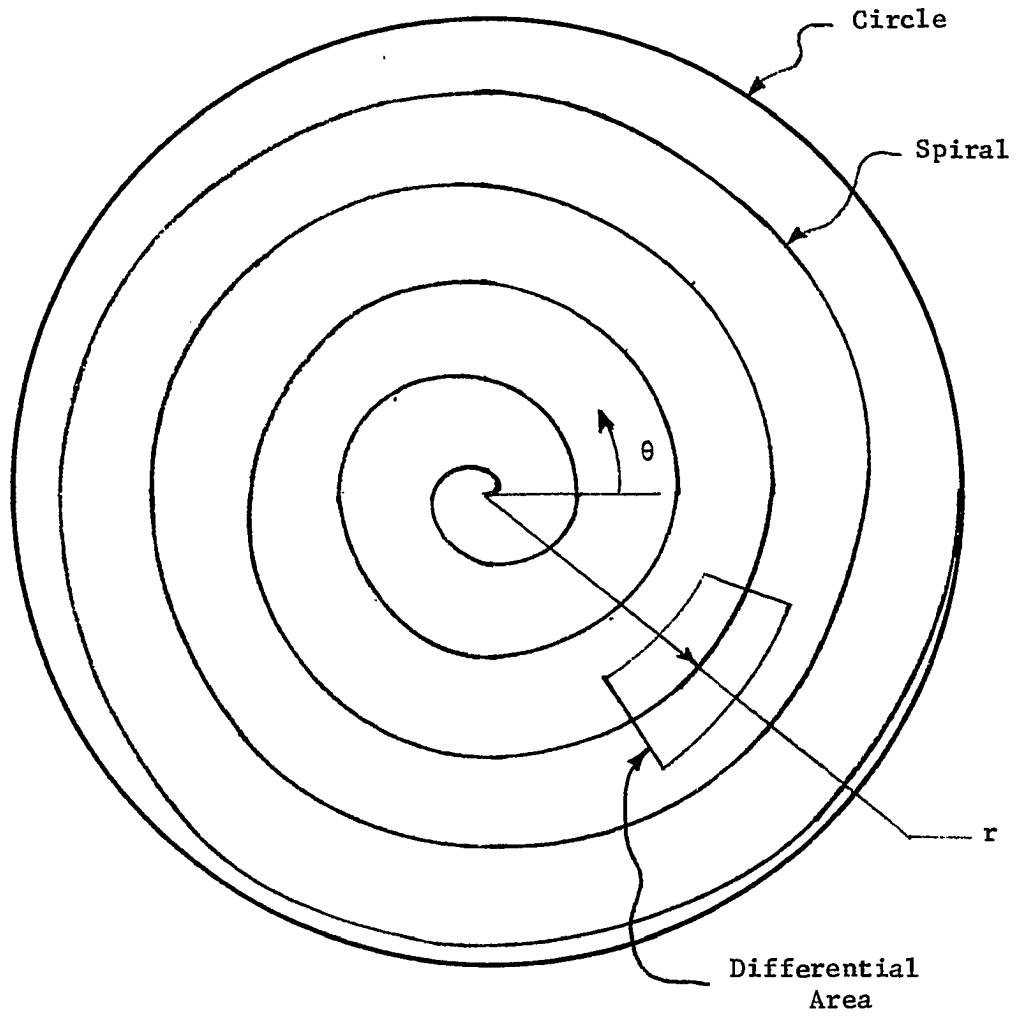


Figure 1. The spiral of Archimedes inscribed within a circle

positions previously occupied by the area.

The differential area used in the formulation of the Laplacian operator is shown in Figure 2 by the dotted region.

For the  $r - \theta$  coordinate system, the Laplacian operator when applied to a function  $F(r, \theta)$  is given as

$$\nabla^2 F(r, \theta) = \frac{1}{r} \frac{\partial}{\partial r} r \frac{\partial}{\partial r} F(r, \theta) + \frac{1}{r^2} \frac{\partial^2 F(r, \theta)}{\partial \theta^2}.$$

Integration of the Laplacian over the differential area then yields

$$\iint_{\text{Region}} \left[ \frac{1}{r} \frac{\partial}{\partial r} r \frac{\partial}{\partial r} F(r, \theta) + \frac{1}{r^2} \frac{\partial^2}{\partial \theta^2} F(r, \theta) \right] r \, dr \, d\theta. \quad (3)$$

This surface integral can be transformed into a line integral by applying Green's lemma:

$$\iint_{\text{Region}} \left[ \frac{\partial V}{\partial x} - \frac{\partial U}{\partial y} \right] dx dy = \oint (U dx + V dy). \quad (4)$$

That is,

$$\begin{aligned} \iint_{\text{Region}} \left[ \frac{1}{r} \frac{\partial}{\partial r} r \frac{\partial F}{\partial r} + \frac{1}{r^2} \frac{\partial^2 F}{\partial \theta^2} \right] r \, dr \, d\theta &= \\ \iint_{\text{Region}} \left[ \frac{\partial}{\partial r} r \frac{\partial F}{\partial r} + \frac{1}{r} \frac{\partial^2 F}{\partial \theta^2} \right] dr \, d\theta &= \\ \oint \left[ -\frac{1}{r} \frac{\partial F}{\partial \theta} dr + r \frac{\partial F}{\partial r} d\theta \right] & \end{aligned} \quad (5)$$

Consideration of the line integration along the curve  $C_1$  between points

$P_1$  and  $P_2$  gives

$$\begin{aligned} \oint_{C_1} \left[ -\frac{1}{r} \frac{\partial F}{\partial \theta} dr + r \frac{\partial F}{\partial r} d\theta \right] &= - \int_{P_1}^{Q_1} \frac{1}{r} \frac{\partial F}{\partial \theta} dr + \int_{P_1}^{Q_1} r \frac{\partial F}{\partial r} d\theta \\ &\quad - \int_{Q_1}^{P_2} \frac{1}{r} \frac{\partial F}{\partial \theta} dr + \int_{Q_1}^{P_2} r \frac{\partial F}{\partial r} d\theta. \end{aligned} \quad (6)$$

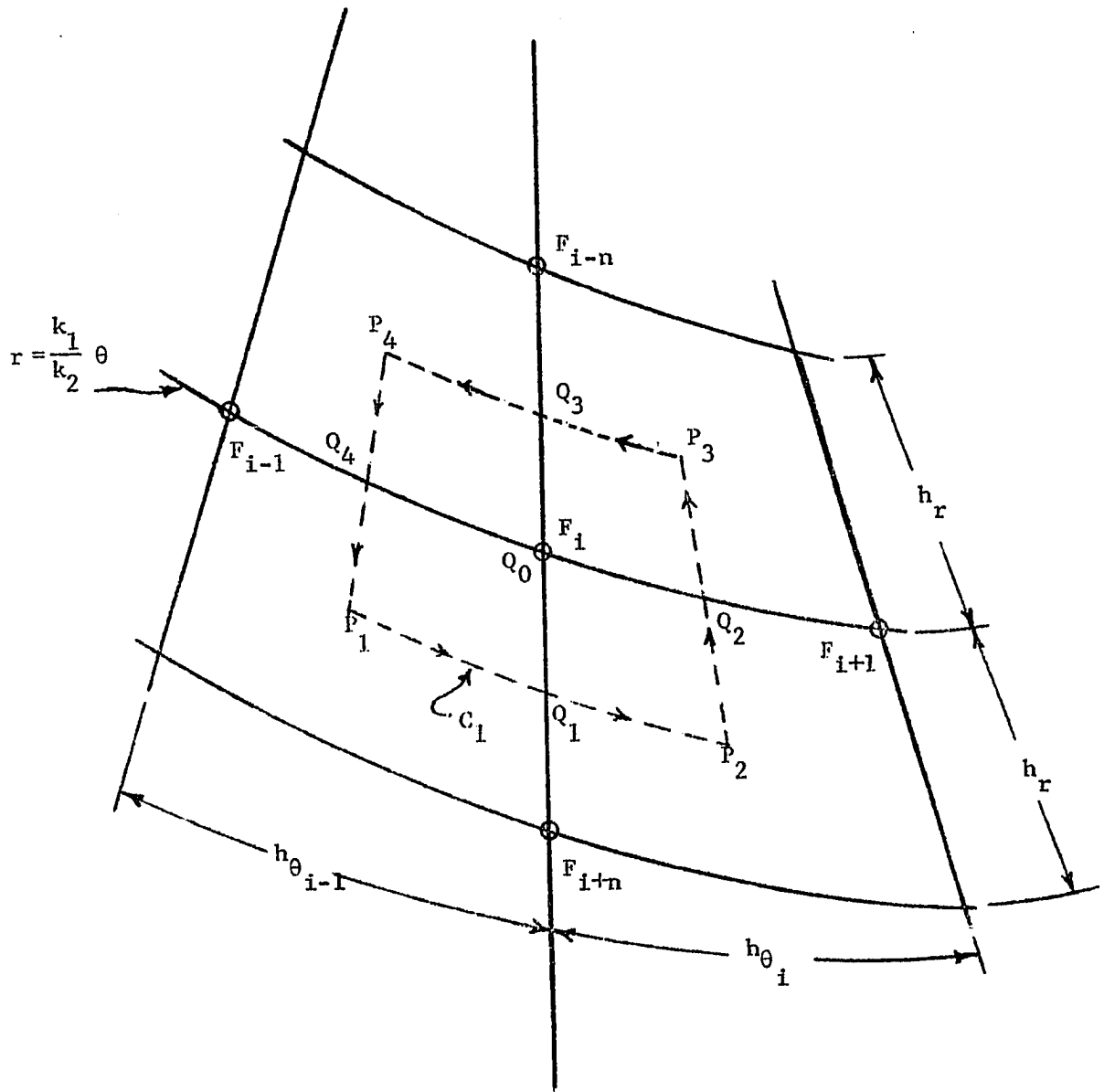


Figure 2. Differential area of  $r - \theta$  parametric system

The general numerical approximations for the integrals in Equation 2 are

$$\int_{r_a}^{r_b} \frac{1}{r} \frac{\partial F}{\partial \theta} dr = \left( \frac{\partial F}{\partial \theta} \right) \int_{r_a}^{r_b} \frac{1}{r} dr = \left( \frac{\partial F}{\partial \theta} \right) \ln \frac{r_b}{r_a} \quad (7)$$

$$\int_{\theta_a}^{\theta_b} r \frac{\partial F}{\partial r} d\theta = \left( \frac{\partial F}{\partial r} \right) \int_{\theta_a}^{\theta_b} \frac{k_1}{k_2} \theta d\theta = \frac{1}{2} \frac{k_1}{k_2} \left( \frac{\partial F}{\partial r} \right) (\theta_b^2 - \theta_a^2). \quad (8)$$

By using a divided difference form for the derivative, Equations 7 and 8 become

$$\int_{r_a}^{r_b} \frac{1}{r} \frac{\partial F}{\partial \theta} dr = \left( \frac{F_{i-1} - F_i}{h_{\theta_{i-1}}} \right) \ln \frac{r_b}{r_a} + O(h^2) \quad (9)$$

$$\int_{\theta_a}^{\theta_b} r \frac{\partial F}{\partial r} d\theta = \left( \frac{F_{i+n} - F_i}{h_{r_i}} \right) \frac{1}{2} \frac{k_1}{k_2} (\theta_b^2 - \theta_a^2) + O(h^2) \quad (10)$$

where  $O(h^2)$  indicates a truncation error of order  $h^2$  has been introduced by the approximation of the derivative. Application of Equations 9 and 10 to Equation 6 gives

$$\begin{aligned} \oint_{C_1} \left[ -\frac{1}{r} \frac{\partial F}{\partial \theta} dr + r \frac{\partial F}{\partial r} d\theta \right] &= -\frac{1}{h_{\theta_{i-1}}} (F_{i-1} - F_i) \ln \frac{r_{Q_1}}{r_{P_1}} \\ &+ \frac{1}{2h_{r_i}} \frac{k_1}{k_2} (F_{i+n} - F_i) (\theta_{P_2}^2 - \theta_{P_1}^2) - \frac{1}{h_{\theta_i}} (F_{i+1} - F_i) \ln \frac{r_{P_2}}{r_{Q_1}} \\ &+ O(h^2) \end{aligned} \quad (11)$$

where

$$\begin{aligned} h_{r_i} &= k_1 \Delta S_{r_i} \\ h_{\theta_{i-1}} &= k_2 \Delta S_{\theta_{i-1}} \end{aligned} \quad (12)$$

The original independent variables are now removed by applying their equivalent functions in  $S$  as given in Equations 1. Equation 11 then becomes

$$\oint_{C_1} \left[ -\frac{1}{r} \frac{\partial F}{\partial \theta} dr + r \frac{\partial F}{\partial r} d\theta \right] = -\frac{1}{k_2 \Delta S_{\theta_{i-1}}} (F_{i-1} - F_i) \ln \frac{S_{Q_1}}{S_{P_2}} + \frac{1}{2} \frac{k_2}{\Delta S_{r_i}} (F_{i+n} - F_i) (S_{P_2}^2 - S_{P_1}^2) - \frac{1}{k_2 \Delta S_{\theta_i}} (F_{i+1} - F_i) \ln \frac{S_{P_2}}{S_{Q_1}} + O(h^2). \quad (13)$$

It is reasonable to assume that the order of the error term will not be decreased by the introduction of the parametric variable.

The same procedures are followed along the path  $P_2 P_3 P_4$ . The values of the function  $F(r, \theta)$  are factored from the sum of the line integrals along all four sides giving the five point formula

$$\begin{aligned} \oint \left[ -\frac{1}{r} \frac{\partial F}{\partial \theta} dr + r \frac{\partial F}{\partial r} d\theta \right] &= \frac{1}{2} \frac{k_2}{\Delta S_{r_i}} (S_{P_2}^2 - S_{P_1}^2) F_{i+n} \\ &- \frac{1}{k_2 \Delta S_{\theta_i}} \ln \frac{S_{Q_3}}{S_{Q_1}} F_{i+1} + \frac{1}{2} \frac{k_2}{\Delta S_{r_{i-1}}} (S_{P_4}^2 - S_{P_3}^2) F_{i-n} \\ &- \frac{1}{k_2 \Delta S_{\theta_{i-1}}} \ln \frac{S_{Q_1}}{S_{Q_3}} F_{i-1} + \left[ -\frac{1}{2} \frac{k_2}{\Delta S_{r_i}} (S_{P_2}^2 - S_{P_1}^2) \right. \\ &+ \frac{1}{k_2 \Delta S_{\theta_i}} \ln \frac{S_{Q_3}}{S_{Q_1}} - \frac{1}{2} \frac{k_2}{\Delta S_{r_{i-1}}} (S_{P_4}^2 - S_{P_3}^2) \\ &\left. + \frac{1}{k_2 \Delta S_{\theta_{i-1}}} \ln \frac{S_{Q_1}}{S_{Q_3}} \right] F_i + O(h^2) \end{aligned} \quad (14)$$

or

$$\oint \left[ -\frac{1}{r} \frac{\partial F}{\partial \theta} dr + r \frac{\partial F}{\partial r} d\theta \right] = \alpha_1 F_{i+n} + \alpha F_{i+1} + \alpha_3 F_{i-n} + \delta F_{i-1} + \beta F_i + O(h^2). \quad (15)$$

where  $\alpha_1$ ,  $\alpha$ ,  $\alpha_3$ ,  $\delta$ , and  $\beta$  in Equation 15 are defined by the corresponding coefficient of  $F$  in Equation 14. Equation 15 is the two-dimensional Laplacian operator in terms of one variable as applied to one differential area of the spiral. Note that this expression is entirely in difference form and is adaptable to a digital computer. A derivative term is needed for effective hybrid computation. For equally spaced  $h_\theta$ ,  $\alpha = \delta$ . From the definition of a total derivative of  $F(r, \theta)$

$$\frac{dF}{dS} = \frac{\partial F}{\partial r} \frac{dr}{dS} + \frac{\partial F}{\partial \theta} \frac{d\theta}{dS} \quad (16)$$

it follows that

$$\frac{dF_i}{dS} = k_1 \left( \frac{F_{i+n} - F_{i-n}}{2h_r} \right) + k_2 \left( \frac{F_{i+1} - F_{i-1}}{2h_\theta} \right) \quad (17)$$

and

$$F_{i+1} = \frac{2h_\theta}{k_2} \left[ \frac{dF}{dS} - k_1 \left( \frac{F_{i+n} - F_{i-n}}{2h_r} \right) \right] + F_{i-1}. \quad (18)$$

Equation 18 is combined with Equation 15 to remove  $F_{i+1}$  and express the line integral in difference and differential form as

$$\begin{aligned} \oint \left[ -\frac{1}{r} \frac{\partial F}{\partial \theta} + r \frac{\partial F}{\partial r} d\theta \right] &= \left( \alpha_1 - \alpha \frac{\Delta S_\theta}{\Delta S_r} \right) F_{i+n} \\ &+ \left( \alpha_3 + \alpha \frac{\Delta S_\theta}{\Delta S_r} \right) F_{i-n} + 2\alpha \Delta S_\theta \frac{dF_i}{dS} + 2\alpha F_{i-1} \\ &+ \left( -\alpha_1 - 2\alpha - \alpha_3 \right) F_i + O(h^2). \end{aligned} \quad (19)$$

On the hybrid computer, the analog portion of the computer would solve for the derivative term using the digital computer for generation of  $\alpha_1$ ,  $\alpha$ ,

$\alpha_3$ , and storage of F for subsequent iterations.

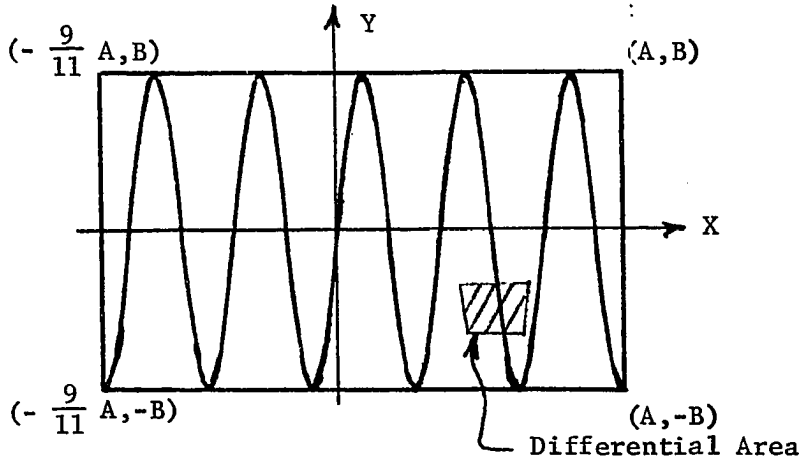
In the application of the related independent variables technique to the Laplacian operator for hybrid computation, only one differential area is considered. This area sweeps through the range of the parametric variable and repeats its movement once for each iteration. A balance equation over the differential area then applies to the total geometry. This technique is applied to Neumann and Dirichlet boundary conditions by changing the limits of the differential area and subsequent integration procedures to match the physical boundary where the condition is prescribed. Physical constants appearing in the balance equations are adjusted before each iteration sweep, and the sweeps are repeated until the boundary conditions are satisfied. The resulting solution of the dependent variable is continuous in S-space and applicable to continuous space, discrete time solutions of time dependent partial differential equations.

For a digital computer, the differential area is stationary and surrounds a grid point. Each differential area in the total geometry introduces an expression like Equation 15. When this technique is applied to problems involving the Laplacian operator, each area introduces an equation. The distribution of  $F(r,\theta)$  is then found by simultaneous solution of these equations, and those arising from boundary conditions, by ordinary digital computer techniques. The procedures for both computers are illustrated in the section showing the application of the related independent variables technique to a nuclear reactor.

In order to apply this method to other geometries the same general steps are followed:

1. Select a parametric function which will relate the independent variables
2. Discretize the space described by the independent variables
3. Integrate over each differential subspace and apply Green's theorem to reduce the number of dimensions involved in the integration
4. Replace the independent variables with their parametric equivalent
5. Apply computer techniques to solve for the dependent variable.

Examples of how this method could be applied to Cartesian, cylindrical, and spherical coordinate systems are shown in the following figures.

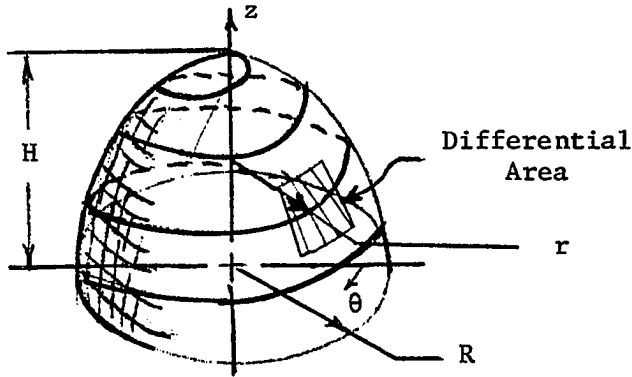


Equations:

$$X = \frac{A}{S_{\max}} S$$

$$Y = B \sin kS$$

Figure 3. Description of a rectangular surface



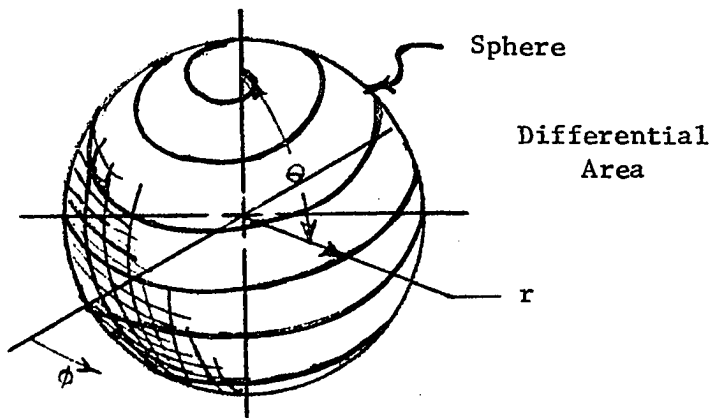
Equations:

$$r = R \sin \frac{\pi}{2} \frac{R}{S_{\max}} S$$

$$\theta = \frac{\theta_{\max}}{S_{\max}} S$$

$$z = \frac{H}{S_{\max}} S$$

Figure 4. Description of a cylindrical surface



Equations:

$$r = \text{constant}$$

$$\theta = \frac{180^\circ}{S_{\max}} S$$

$$\phi = \frac{\phi_{\max}}{S_{\max}} S$$

Figure 5. Description of a spherical surface

### III. APPLICATION TO A NUCLEAR REACTOR

In this section, the methods used in the derivation of the parametric Laplacian operator are applied to a nuclear reactor, and the equations for both digital and hybrid computer solutions of the steady state flux distribution are presented. The polar geometry considered in this example is relevant to the description of several reactor problems. The spatial distribution of fission products such as xenon and of burnable poisons as well as the effects of control rod position and other localized reactivity perturbations are a few of the topics related to the study of azimuthal flux distribution in a cylindrical reactor core.

The two-dimensional diffusion equation, applied to an infinite cylindrical reactor, is

$$\frac{1}{r} \frac{\partial}{\partial r} r D(r, \theta) \frac{\partial \phi}{\partial r} + \frac{1}{r^2} \frac{\partial}{\partial \theta} D(r, \theta) \frac{\partial \phi(r, \theta)}{\partial \theta} + \nu \Sigma_f(r, \theta) \phi(r, \theta) - \Sigma_a(r, \theta) \phi(r, \theta) = 0 \quad (20)$$

where

$r$  denotes radial space dependence.

$\theta$  denotes angular space dependence.

$\phi$  is the neutron flux.

$D$  is the diffusion coefficient.

$\Sigma_a$  is a macroscopic absorption cross section.

$\nu$  is the average number of neutrons released by fission.

$\Sigma_f$  is a macroscopic fission cross section.

The best parametric relationship for this geometry is the spiral of Archimedes given as

$$\begin{aligned} r &= k_1 S \\ \theta &= k_2 S. \end{aligned} \quad (21)$$

Integration of Equation 20 over the area of the spiral segment shown in Figure 6 gives

$$\iint_{R_1, R_2, R_3, R_4} \left[ \frac{1}{r} \frac{\partial}{\partial r} r D \frac{\partial \phi}{\partial r} + \frac{1}{r^2} \frac{\partial}{\partial \theta} D \frac{\partial \phi}{\partial \theta} + \nu \Sigma_f \phi - \Sigma_a \phi \right] r dr d\theta = 0. \quad (22)$$

Consideration will first be given to the first two terms describing the leakage with the requirement that each of the four regions be homogeneous.

The leakage term is then expressed as

$$\iint_{\substack{R_1, R_2, \\ R_3, R_4}} \frac{1}{r} \frac{\partial}{\partial r} r D \frac{\partial \phi}{\partial r} + \frac{1}{r^2} \frac{\partial}{\partial \theta} D \frac{\partial \phi}{\partial \theta} r dr d\theta = \sum_{k=1}^4 D_k \iint_{R_k} \left[ \frac{\partial}{\partial r} r \frac{\partial \phi}{\partial r} + \frac{1}{r} \frac{\partial}{\partial \theta} \frac{\partial \phi}{\partial \theta} \right] dr d\theta. \quad (23)$$

Green's lemma is applied to transform the surface integral over a region to a line integral.

$$\iint \left[ \frac{\partial}{\partial r} r \frac{\partial \phi}{\partial r} + \frac{1}{r} \frac{\partial}{\partial \theta} \frac{\partial \phi}{\partial \theta} \right] dr d\theta = \oint \left[ -\frac{1}{r} \frac{\partial \phi}{\partial \theta} dr + r \frac{\partial \phi}{\partial r} d\theta \right] \quad (24)$$

Application of Equation 24 to  $R_1$  gives

$$\begin{aligned} D_1 \iint_{R_1} \left[ \frac{\partial}{\partial r} r \frac{\partial \phi}{\partial r} + \frac{1}{r} \frac{\partial^2 \phi}{\partial \theta^2} \right] dr d\theta &= D_1 \int_{\theta_{P_1}}^{\theta_{Q_1}} r \frac{\partial \phi}{\partial r} d\theta - D_1 \int_{r_{P_1}}^{r_{Q_1}} \frac{1}{r} \frac{\partial \phi}{\partial \theta} dr \\ &+ D_1 \int_{\theta_{Q_1}}^{\theta_{Q_0}} r \frac{\partial \phi}{\partial r} d\theta - D_1 \int_{r_{Q_1}}^{r_{Q_0}} \frac{1}{r} \frac{\partial \phi}{\partial \theta} dr + D_1 \int_{\theta_{Q_0}}^{\theta_{Q_4}} r \frac{\partial \phi}{\partial r} d\theta - D_1 \int_{r_{Q_0}}^{r_{Q_4}} \frac{1}{r} \frac{\partial \phi}{\partial \theta} dr \\ &+ D_1 \int_{\theta_{Q_4}}^{\theta_{P_1}} r \frac{\partial \phi}{\partial r} d\theta - D_1 \int_{r_{Q_4}}^{r_{P_1}} \frac{1}{r} \frac{\partial \phi}{\partial \theta} dr. \end{aligned} \quad (25)$$

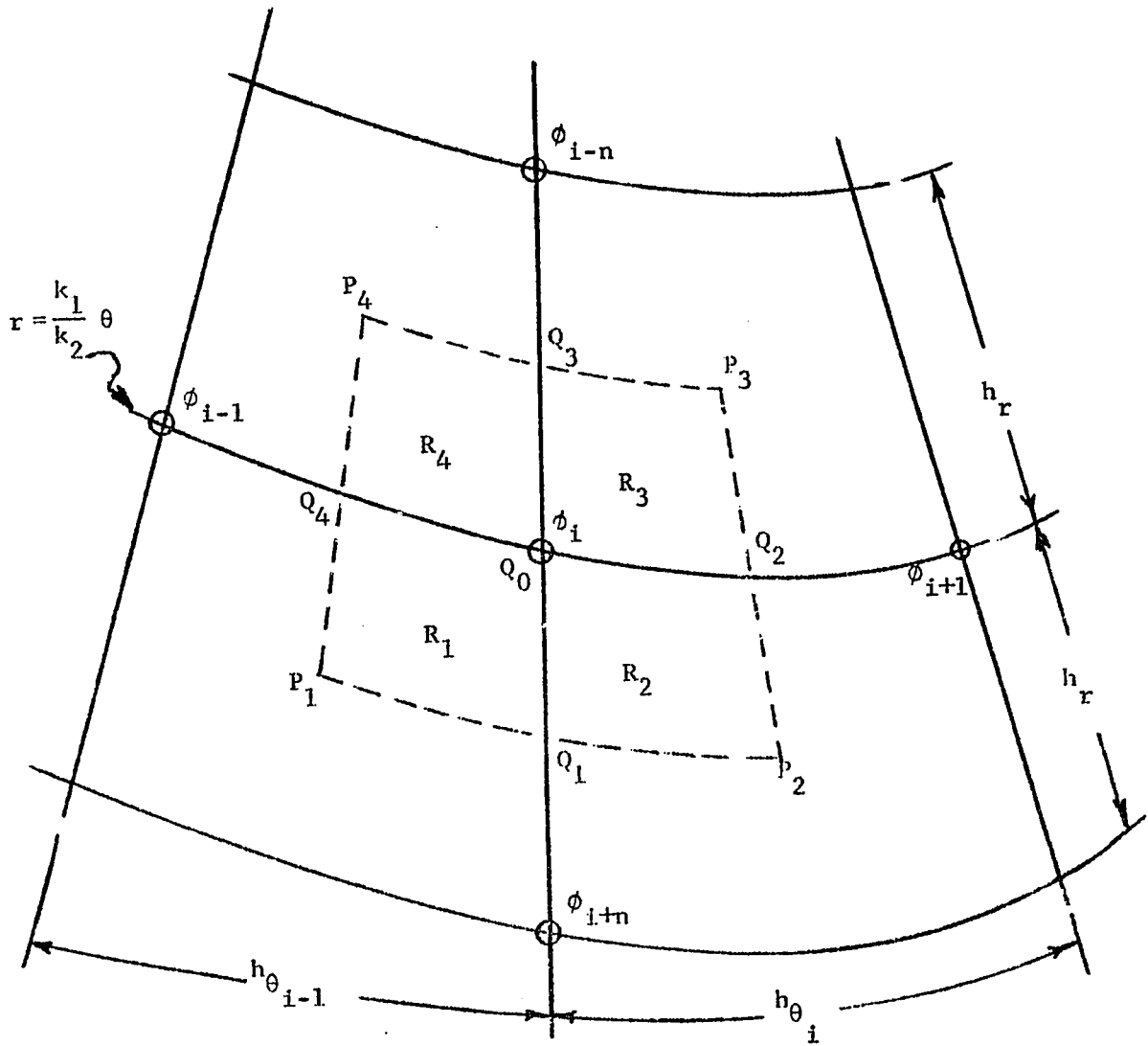


Figure 6. Differential reactor area

It appears that when considering all four regions there will be a line-integral into the center point and out again, so that between neighboring regions the sum of the line integration in and out is as follows.

$$\begin{aligned}
 & D_1 \int_{\theta_{Q_1}}^{\theta_{Q_0}} r \frac{\partial \phi}{\partial r} d\theta - D_1 \int_{r_{Q_1}}^{r_{Q_0}} \frac{1}{r} \frac{\partial \phi}{\partial \theta} dr + D_2 \int_{\theta_{Q_0}}^{\theta_{Q_1}} r \frac{\partial \phi}{\partial r} d\theta - D_2 \int_{r_{Q_0}}^{r_{Q_1}} \frac{1}{r} \frac{\partial \phi}{\partial \theta} dr = \\
 & \int_{r_{Q_0}}^{r_{Q_1}} r \left( D_2 \frac{\partial \phi}{\partial r} - D_1 \frac{\partial \phi}{\partial r} \right) dr - \int_{\theta_{Q_0}}^{\theta_{Q_1}} \frac{1}{r} \left( D_2 \frac{\partial \phi}{\partial \theta} - D_1 \frac{\partial \phi}{\partial \theta} \right) d\theta \quad (26)
 \end{aligned}$$

When the continuity of current relationship,

$$D_k \frac{\partial \phi}{\partial n} = D_j \frac{\partial \phi}{\partial n} \quad (27)$$

is applied at each region interface, the bracketed term is seen to be zero. Therefore the total effect of the integration over all four regions is the line integral along the dotted line  $P_1Q_1P_2Q_2P_3Q_3P_4Q_4P_1$ . This means

$$\begin{aligned}
& \sum_{k=1}^4 D_k \iint_{R_k} \left[ \frac{\partial}{\partial r} r \frac{\partial \phi}{\partial r} + \frac{1}{r} \frac{\partial^2 \phi}{\partial \theta^2} \right] dr d\theta = \\
& D_1 \int_{\theta_{P_1}}^{\theta_{Q_1}} r \frac{\partial \phi}{\partial r} d\theta - D_1 \int_{r_{P_1}}^{r_{Q_1}} \frac{1}{r} \frac{\partial \phi}{\partial \theta} dr + D_2 \int_{\theta_{Q_1}}^{\theta_{P_2}} r \frac{\partial \phi}{\partial r} d\theta - D_2 \int_{r_{Q_1}}^{r_{P_2}} \frac{1}{r} \frac{\partial \phi}{\partial \theta} dr \\
& + D_2 \int_{\theta_{P_2}}^{\theta_{Q_2}} r \frac{\partial \phi}{\partial r} d\theta - D_2 \int_{r_{P_2}}^{r_{Q_2}} \frac{1}{r} \frac{\partial \phi}{\partial \theta} dr + D_3 \int_{\theta_{Q_2}}^{\theta_{P_3}} r \frac{\partial \phi}{\partial r} d\theta - D_3 \int_{r_{Q_2}}^{r_{P_3}} \frac{1}{r} \frac{\partial \phi}{\partial \theta} dr \\
& + D_3 \int_{\theta_{P_3}}^{\theta_{Q_3}} r \frac{\partial \phi}{\partial r} d\theta - D_3 \int_{r_{P_3}}^{r_{Q_3}} \frac{1}{r} \frac{\partial \phi}{\partial \theta} dr + D_4 \int_{\theta_{Q_3}}^{\theta_{P_4}} r \frac{\partial \phi}{\partial r} d\theta - D_4 \int_{r_{Q_3}}^{r_{P_4}} \frac{1}{r} \frac{\partial \phi}{\partial \theta} dr \\
& + D_4 \int_{\theta_{P_4}}^{\theta_{Q_4}} r \frac{\partial \phi}{\partial r} d\theta - D_4 \int_{r_{P_4}}^{r_{Q_4}} \frac{1}{r} \frac{\partial \phi}{\partial \theta} dr + D_1 \int_{\theta_{Q_4}}^{\theta_{P_1}} r \frac{\partial \phi}{\partial r} d\theta - D_1 \int_{r_{Q_4}}^{r_{P_1}} \frac{1}{r} \frac{\partial \phi}{\partial \theta} dr .
\end{aligned} \tag{28}$$

When the relationship  $r = \frac{k_1}{k_2} \theta$  is used, the two types of integrals in the above expression are approximated as follows.

$$\int_{r_a}^{r_b} \frac{1}{r} \frac{\partial \phi}{\partial \theta} dr = \left( \frac{\partial \phi}{\partial \theta} \right) \int_{r_a}^{r_b} \frac{1}{r} dr = \left( \frac{\partial \phi}{\partial \theta} \right) \ln \frac{r_b}{r_a} \tag{29}$$

$$\int_{\theta_a}^{\theta_b} r \frac{\partial \phi}{\partial r} d\theta = \left( \frac{\partial \phi}{\partial r} \right) \int_{\theta_a}^{\theta_b} \frac{k_1}{k_2} \theta d\theta = \frac{1}{2} \frac{k_1}{k_2} \left( \frac{\partial \phi}{\partial r} \right) (\theta_b^2 - \theta_a^2) \tag{30}$$

When the divided difference form is used for the derivative and the parametric equations of the  $r$  and  $\theta$  variables given in Equation 21 are substituted into the two integral expressions above, the resulting integral expressions are as follows.

$$\int_{r_a}^{r_b} \frac{1}{r} \frac{\partial \phi}{\partial \theta} dr = \frac{1}{k_2 \Delta S_{\theta ab}} (\phi_b - \phi_a) \ln \frac{S_b}{S_a} + O(h^2) \quad (31)$$

$$\int_{\theta_a}^{\theta_b} r \frac{\partial \phi}{\partial r} d\theta = \frac{k_2}{2 \Delta S_{rab}} (\phi_b - \phi_a) (S_b^2 - S_a^2) + O(h^2) \quad (32)$$

The above expressions are then used in Equation 28. After collecting terms for all four regions and factoring, the five point formula for the leakage term is as follows.

$$\begin{aligned}
& \sum_{k=1}^4 D_k \iint_{R_k} \left[ \frac{\partial}{\partial r} r \frac{\partial \phi}{\partial r} + \frac{1}{r} \frac{\partial^2 \phi}{\partial \theta^2} \right] dr d\theta = \\
& \quad \frac{k_2}{2h_{r_i}} \left[ D_1 (S_{Q_1}^2 - S_{P_1}^2) + D_2 (S_{P_2}^2 - S_{Q_1}^2) \right] \phi_{i+n} \\
& \quad + \left\{ -\frac{1}{k_2 h_{\theta_i}} \left[ D_2 \ln \frac{S_{Q_2}}{S_{Q_1}} + D_3 \ln \frac{S_{Q_3}}{S_{Q_2}} \right] \right\} \phi_{i+1} \\
& \quad + \left\{ -\frac{k_2}{2h_{r_{i-1}}} \left[ D_3 (S_{Q_3}^2 - S_{P_3}^2) + D_4 (S_{P_4}^2 - S_{Q_3}^2) \right] \right\} \phi_{i-n} \\
& \quad + \left\{ \frac{1}{k_2 h_{\theta_{i-1}}} \left[ D_4 \ln \frac{S_{Q_4}}{S_{Q_3}} + D_1 \ln \frac{S_{Q_1}}{S_{Q_4}} \right] \right\} \phi_{i-1} \\
& \quad + \left\{ -\frac{k_2}{2h_{r_i}} \left[ D_1 (S_{Q_1}^2 - S_{P_1}^2) + D_2 (S_{P_2}^2 - S_{Q_1}^2) \right] \right. \\
& \quad + \frac{1}{k_2 h_{\theta_i}} \left[ D_2 \ln \frac{S_{Q_2}}{S_{Q_1}} + D_3 \ln \frac{S_{Q_3}}{S_{Q_2}} \right] \\
& \quad + \frac{k_2}{2h_{r_{i-1}}} \left[ D_3 (S_{Q_3}^2 - S_{P_3}^2) + D_4 (S_{P_4}^2 - S_{Q_3}^2) \right] \\
& \quad \left. - \frac{1}{k_2 h_{\theta_{i-1}}} \left[ D_4 \ln \frac{S_{Q_4}}{S_{Q_3}} + D_1 \ln \frac{S_{Q_1}}{S_{Q_4}} \right] \right\} \phi_i + o(h^2) \tag{33}
\end{aligned}$$

By defining the coefficients on  $\phi_{i+n}$ ,  $\phi_{i+1}$ ,  $\phi_{i-n}$ , and  $\phi_{i-1}$  as  $\alpha_1$ ,  $\alpha$ ,  $\alpha_3$ , and  $\delta$  respectively, Equation 33 can be written simply as

$$\alpha_1 \phi_{i+n} + \alpha \phi_{i+1} + \alpha_3 \phi_{i-n} + \delta \phi_{i-1} + (-\alpha_1 - \alpha - \alpha_3 - \delta) \phi_i + o(h^2) \tag{34}$$

This expression would be applied to a digital computer for it does not contain a derivative. For hybrid application, a derivative term is formulated as follows. Recall from consideration of the total derivative that for equal azimuthal spacing it was shown in Equation 18 that

$$\phi_{i+1} = \frac{2h_\theta}{k_2} \left[ \frac{d\phi_i}{dS} - k_1 \left( \frac{\phi_{i+n} - \phi_{i-n}}{2h_r} \right) \right] + \phi_{i-1}. \quad (35)$$

Equation 34 now becomes

$$\begin{aligned} & \left( \alpha_1 - \alpha \frac{\Delta S_\theta}{\Delta S_r} \right) \phi_{i+n} + 2\Delta S_\theta \alpha \frac{d\phi_i}{dS} + \left( \alpha_3 + \alpha \frac{\Delta S_\theta}{\Delta S_r} \right) \phi_{i-n} \\ & + (\delta + 2\Delta S_\theta \alpha) \phi_{i-1} + (-\alpha_1 - 2\alpha - \alpha_3) + O(h^2) \end{aligned} \quad (36)$$

which is applicable to a hybrid computer.

Next consider the source and absorption terms in Equation 20. It is stipulated that material properties are not space dependent within regions and assumed that the flux at the center point is the average flux within the regions so that

$$\iint_{R_1, R_2, R_3, R_4} (\nu \Sigma_f - \Sigma_a) \phi_i r \, dr \, d\theta = \sum_{k=1}^4 (\nu \Sigma_{f_k} - \Sigma_{a_k}) \phi_i \iint_{R_k} r \, dr \, d\theta. \quad (37)$$

The integral term in Equation 37 is the surface area of each region  $A_k$ .

Equation 37 is then written as

$$\iint_{R_1, R_2, R_3, R_4} (\nu \Sigma_f - \Sigma_a) \phi_i r \, dr \, d\theta = \sum_{k=1}^4 (\nu \Sigma_{f_k} - \Sigma_{a_k}) A_k \phi_i. \quad (38)$$

The area of region 3 is determined as follows. From Figure 7,

$$A_3 = \int_{\theta_i}^{\theta_i + \frac{\Delta\theta_i}{2}} \int_{r_i - \frac{\Delta r_i}{2}}^{r_i} r \, dr \, d\theta = \frac{1}{2} \int_{\theta_i}^{\theta_i + \frac{\Delta\theta_i}{2}} \left( \Delta r_i r_i - \frac{\Delta r_i^2}{4} \right) d\theta \quad (39)$$

Noting that  $r = \frac{k_1}{k_2} \theta$ ,

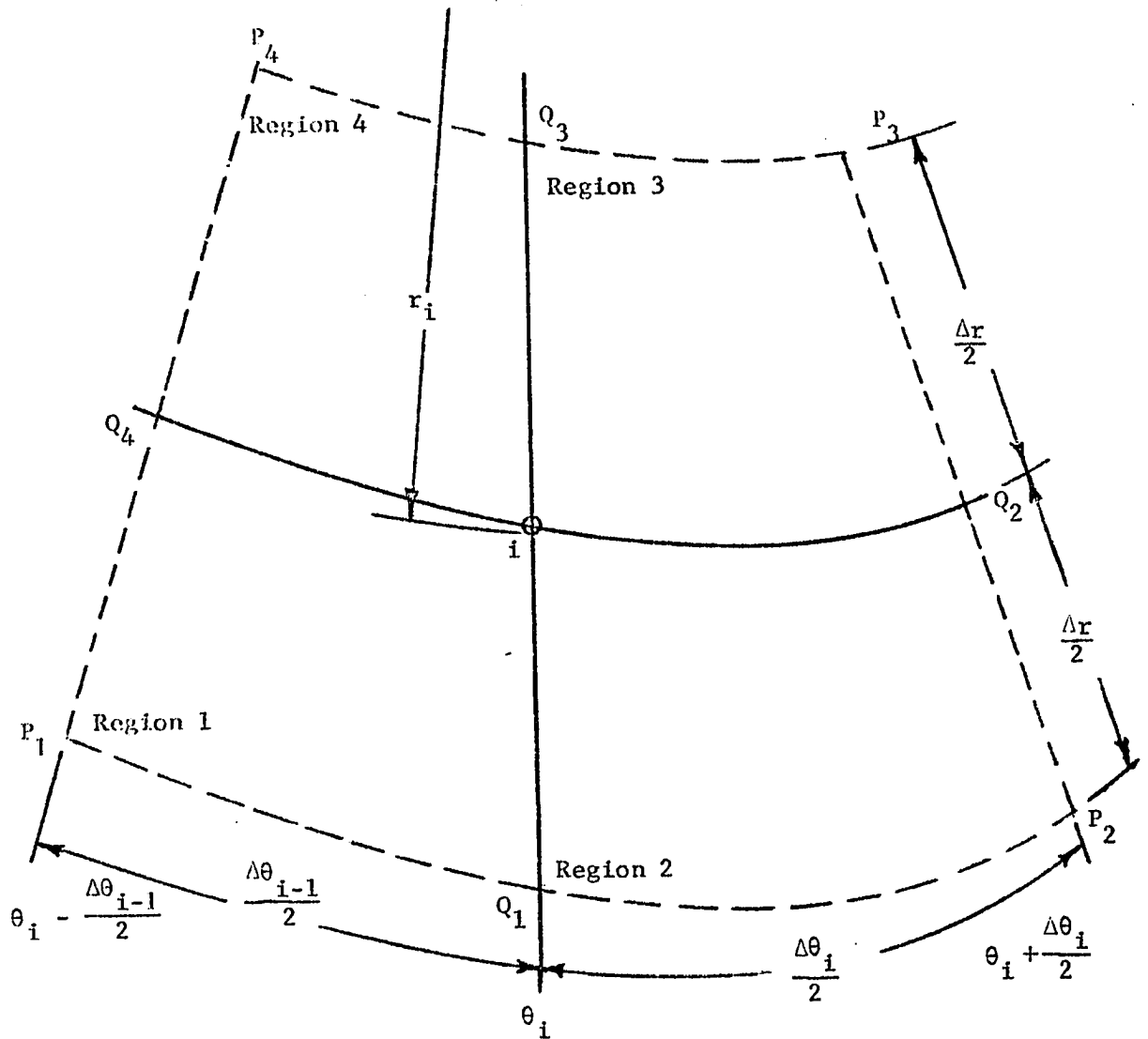


Figure 7. Notation used for determining area of differential regions

$$A_3 = \frac{1}{2} \int_{\theta_i}^{\theta_i + \frac{\Delta\theta_i}{2}} \left( \Delta r_i \frac{k_1}{k_2} \theta_i - \frac{\Delta r_i^2}{4} \right) d\theta = \frac{1}{2} \left[ \frac{k_1}{k_2} \frac{\Delta r_i}{2} \Delta\theta_i \theta_i + \frac{\Delta\theta_i^2}{4} - \frac{\Delta r_i^2}{4} \frac{\Delta\theta_i}{2} \right]. \quad (40)$$

Removal of the variables  $r$  and  $\theta$  by substituting their parametric equivalents gives

$$A_3 = \frac{1}{4} k_1^2 k_2 \Delta S_r \Delta S_\theta \left[ S + \frac{1}{4} (\Delta S_\theta - \Delta S_r) \right]. \quad (41)$$

The areas of the other three regions are found in like manner. They are

$$A_1 = \frac{1}{4} k_1^2 k_2 \Delta S_r \Delta S_{\theta_{i-1}} \left[ S + \frac{1}{4} (\Delta S_r - \Delta S_{\theta_{i-1}}) \right] \quad (42)$$

$$A_2 = \frac{1}{4} k_1^2 k_2 \Delta S_r \Delta S_\theta \left[ S + \frac{1}{4} (\Delta S_\theta + \Delta S_r) \right] \quad (43)$$

$$A_4 = \frac{1}{4} k_1^2 k_2 \Delta S_r \Delta S_{\theta_{i-1}} \left[ S - \frac{1}{4} (\Delta S_r + \Delta S_{\theta_{i-1}}) \right]. \quad (44)$$

Collection of the leakage, source, and absorption terms from all four regions yields the one group diffusion equations for the hybrid and digital computers which follow.

Hybrid:

$$\begin{aligned} & \left( \alpha_1 - \alpha \frac{\Delta S_\theta}{\Delta S_r} \right) \phi_{i+n} + \left( \alpha_3 + \alpha \frac{\Delta S_\theta}{\Delta S_r} \right) \phi_{i-n} + (\delta + 2\alpha \Delta S_\theta) \phi_{i-1} \\ & + 2\alpha \Delta S_\theta \frac{d\phi_i}{dS} + (-\alpha_1 - \alpha - \alpha_3 - \delta) \phi_i + \sum_{k=1}^4 (v \Sigma_{f_k} - \Sigma_{a_k}) A_k \phi_i = 0 \end{aligned} \quad (45)$$

Digital:

$$\begin{aligned} & \alpha_1 \phi_{i+n} + \alpha \phi_{i+1} + \alpha_3 \phi_{i-n} + \delta \phi_{i-1} \\ & + [-\alpha_1 - \alpha - \alpha_3 - \delta + \sum_{k=1}^4 (v \Sigma_{f_k} - \Sigma_{a_k}) A_k] \phi_i = 0 \end{aligned} \quad (46)$$

An inherent limitation of the related independent variables technique is that interfaces between different material regions must coincide with interfaces of the differential areas so that current continuity is maintained and the path traced by the parametric variable can describe material boundaries. This limitation does not affect material interfaces that are described by lines of constant  $\theta$  because two sides of the differential area are formed by rays of the  $r - \theta$  system. Interfaces lying along archs of constant  $r$ , however, must be approximated by the spiral path. For large values of the angular velocity relative to the radial velocity this approximation does not appear to seriously alter the geometry or the results. This will be shown in Section VI.

To account for boundary conditions at the center and outside edges of the reactor, the differential area is modified at the beginning and end of the spiral. For the first revolution, the points  $P_3$ ,  $Q_3$ , and  $P_4$  all fall upon the center point of the reactor,  $r = 0$ . In order to evaluate logarithmic ratio terms, a small finite radius  $r_c$  is drawn about the center. Along the path of this circle,  $r$  is constant but  $\theta$  is a variable. It is therefore necessary to modify the differential region to the region shown in Figure 8. In this case,

$$\int_{\theta_{P_3}}^{\theta_{P_4}} r \frac{\partial \phi}{\partial r} d\theta = r \left( \frac{\partial \phi}{\partial r} \right) (\theta_{P_4} - \theta_{P_3}), \quad (47)$$

and the area of the differential region is found to be

$$A_k = \frac{1}{2} \left[ \frac{1}{3} \frac{k_1^2}{k_2} (\theta_2^3 - \theta_1^3) - r_c^2 \Delta\theta \right]. \quad (48)$$

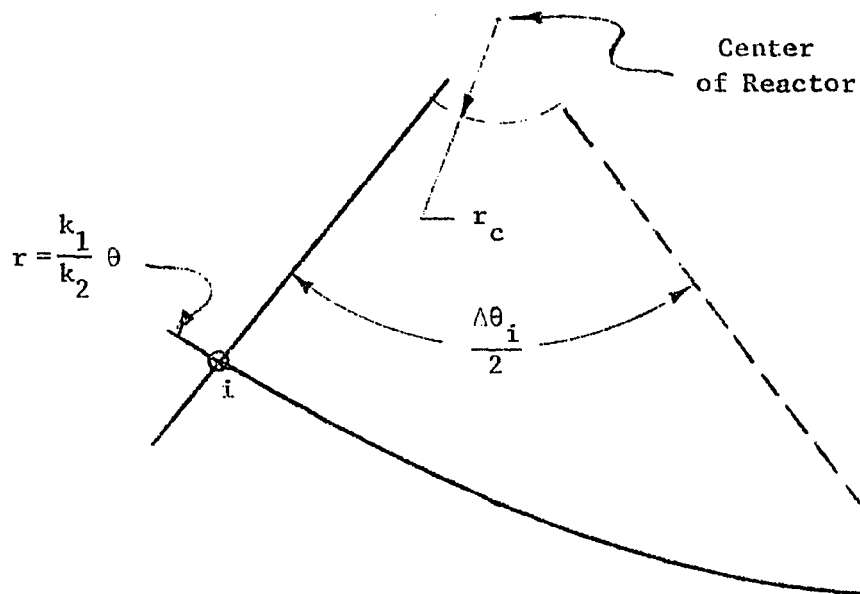


Figure 8. Differential area for first revolution

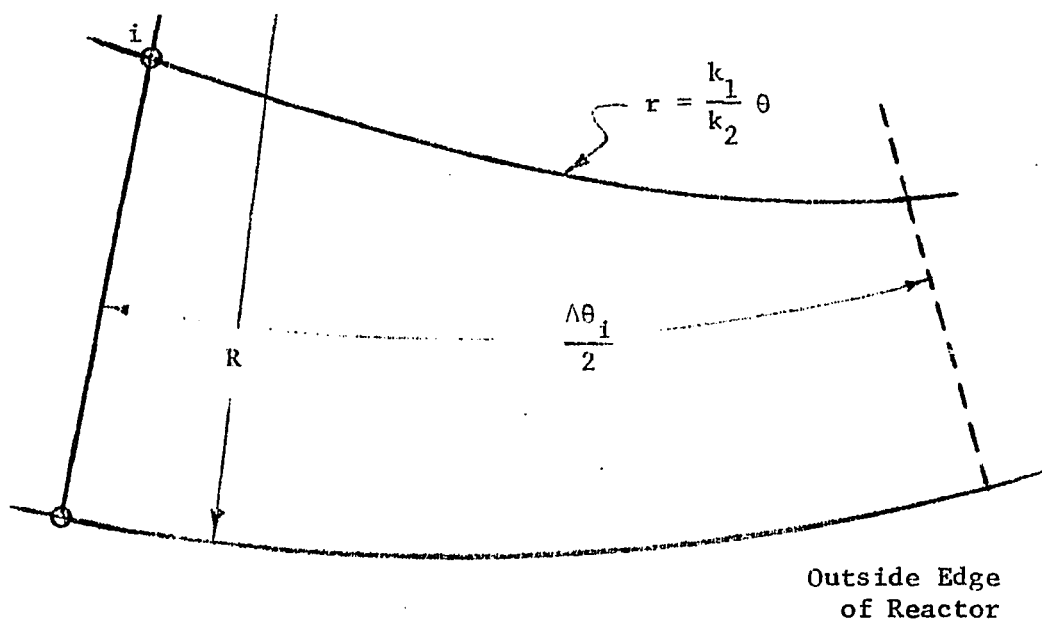


Figure 9. Differential area for last revolution

The initial direction the spiral traces from the center is selected to reduce the error in the solution resulting from the approximation of  $\frac{d\phi}{dS}\Big|_{S=0}$ . When the initial angle  $\theta = 0^\circ$  is parallel or perpendicular to an axis of geometric symmetry of material regions, in the derivative

$$\frac{d\phi}{dS}\Big|_{S=0} = k_1 \frac{\partial\phi}{\partial r}\Big|_{r=0} + k_2 \frac{\partial\phi}{\partial\theta}\Big|_{\theta=0},$$

one of the two partial derivatives on the right hand side is zero, thus simplifying the problem of approximating and visualizing  $\frac{d\phi}{dS}\Big|_{S=0}$ . When the geometry and  $\theta = 0^\circ$  direction are oriented so that  $\frac{d\phi}{dS}\Big|_{S=0}$  is minimized, with or without geometric symmetry, the effect of an error in  $\frac{d\phi}{dS}\Big|_{S=0}$  on the solution is also minimized.

If the value of  $\frac{\partial\phi}{\partial r}$  or  $\frac{\partial\phi}{\partial\theta}$  is specified at the centermost differential area this value would be assigned to the appropriate derivative term of Equation 28. The boundary conditions thus affect the solution through the coefficients of Equations 34 and 36.

As the spiral nears the physical boundary of the reactor on its last revolution, the differential must again be modified. In this case, points  $P_1$ ,  $Q_1$ , and  $P_2$  are moved to fall along the reactor boundary. Here  $r$  is constant and  $\theta$  is a variable. The modified region is shown in Figure 9. For constant  $r$ , the line integral from  $P_1$  and  $P_2$  is then

$$\int_{\theta_{P_1}}^{\theta_{P_2}} r \frac{\partial\phi}{\partial r} d\theta = r \left( \frac{\partial\phi}{\partial r} \right) (\theta_{P_2} - \theta_{P_1}), \quad (49)$$

and the area of the differential region is

$$A = \frac{1}{2} \left[ R^2 \Delta\theta - \frac{1}{3} \frac{k_1^2}{k_2} (\theta_2^3 - \theta_1^3) \right]. \quad (50)$$

Dirichlet boundary conditions are applied by assigning a given flux value to all points along the reactor boundary. For a bare cylindrical reactor the flux is usually considered to be zero at an extrapolated boundary and the derivative at the physical boundary approximated as

$$\left. \frac{\partial \phi}{\partial r} \right|_{r=R} \approx -\frac{3}{2} \frac{1}{\lambda_t} \phi \Big|_{r=R} \quad (51)$$

where  $\lambda_t$  is the transport mean free path. This and other Neumann boundary conditions can be applied by proper specification in Equation 28.

IV. PRESENTATION OF A HYBRID COMPUTER METHOD FOR SOLVING  
MULTIDIMENSIONAL DIFFUSION PROBLEMS

In the last section, the hybrid and digital computer equations describing the diffusion equation were derived. In this section, the general approach to a hybrid computer solution will be outlined. It should be noted that the material here is only a proposal and hybrid computer solution was not made for lack of a hybrid facility. The foundations for the transformation of several space variables to a single variable have, however, been tested using a digital computer and this procedure and results are shown in the following sections.

The first step in the application of the related independent variables technique to the hybrid computer is to write Equation 45 in a form acceptable to analog computation.

$$\begin{aligned}
 \frac{d\phi_i}{dS} + \frac{1}{2\alpha\Delta S_\theta} [(-\alpha_1 - \alpha - \alpha_3 - \delta) + \sum_{k=1}^4 (\nu\Sigma_{f_k} - \Sigma_{a_k})A_k] \phi_i \\
 + \frac{1}{2\alpha\Delta S_\theta} \left( \alpha_1 - \alpha \frac{\Delta S_\theta}{\Delta S_r} \right) \phi_{i+n} + \frac{1}{2\alpha\Delta S_\theta} \left( \alpha_3 + \alpha \frac{\Delta S_\theta}{\Delta S_r} \right) \phi_{i-n} \\
 + \frac{1}{2\alpha\Delta S_\theta} (\delta + 2\alpha\Delta S_\theta) \phi_{i-1} = 0
 \end{aligned} \tag{52}$$

In order to simplify this expression, the following functions are defined

$$\begin{aligned}
P_1(S) &= \frac{1}{2\alpha\Delta S_\theta} [(-\alpha_1 - \alpha - \alpha_3 - \delta) + \sum_{k=1}^4 (\nu\Sigma_{f_k} - \Sigma_a)A_k] \\
P_2(S) &= \frac{1}{2\alpha\Delta S_\theta} \left[ \left( \alpha_1 - \alpha \frac{\Delta S_\theta}{\Delta S_r} \right) \phi_{i+n}^{j-1} + \left( \alpha_3 + \alpha \frac{\Delta S_\theta}{\Delta S_r} \right) \phi_{i-n}^{j-1} \right] \\
P_3(S) &= \frac{\delta}{2\alpha\Delta S_\theta} + 1
\end{aligned} \tag{53}$$

where the superscript  $j-1$  denotes the index of the iteration sweep so that  $\phi_{i+n}^{j-1}$  and  $\phi_{i-n}^{j-1}$  are the flux values at points  $i+n$  and  $i-n$ , shown in Figure 6, of the previous iteration sweep,  $j-1$ . Equation 52 is then simply written

$$\frac{d\phi_i^j}{dS} + P_1(S)\phi_i^j + P_2(S) + P_3(S)\phi_{i-1}^j = 0. \tag{54}$$

The independent variable  $S$  must be available as input to function generators, so it is separated from Equation 54.

Let

$$\frac{dt'}{dS} = m \tag{55}$$

where

$t'$  is the time variable of the analog computer and

$m$  is the constant expressing the rate of change of  $S$  with computer time.

If Equation 54 is divided by Equation 55 the result is

$$\frac{d\phi_i^j}{dt'} + \frac{1}{m} P_1(S)\phi_i^j + \frac{1}{m} P_2(S) + \frac{1}{m} P_3(S)\phi_{i-1}^j = 0. \tag{56}$$

Equations 55 and 56 are programmed for the analog computer. A typical schematic diagram for this method is shown in Figure 10.

The functions  $P_1(S)$ ,  $P_2(S)$ , and  $P_3(S)$  could be produced by function generators using one of two methods. In either method, Equations 53 and

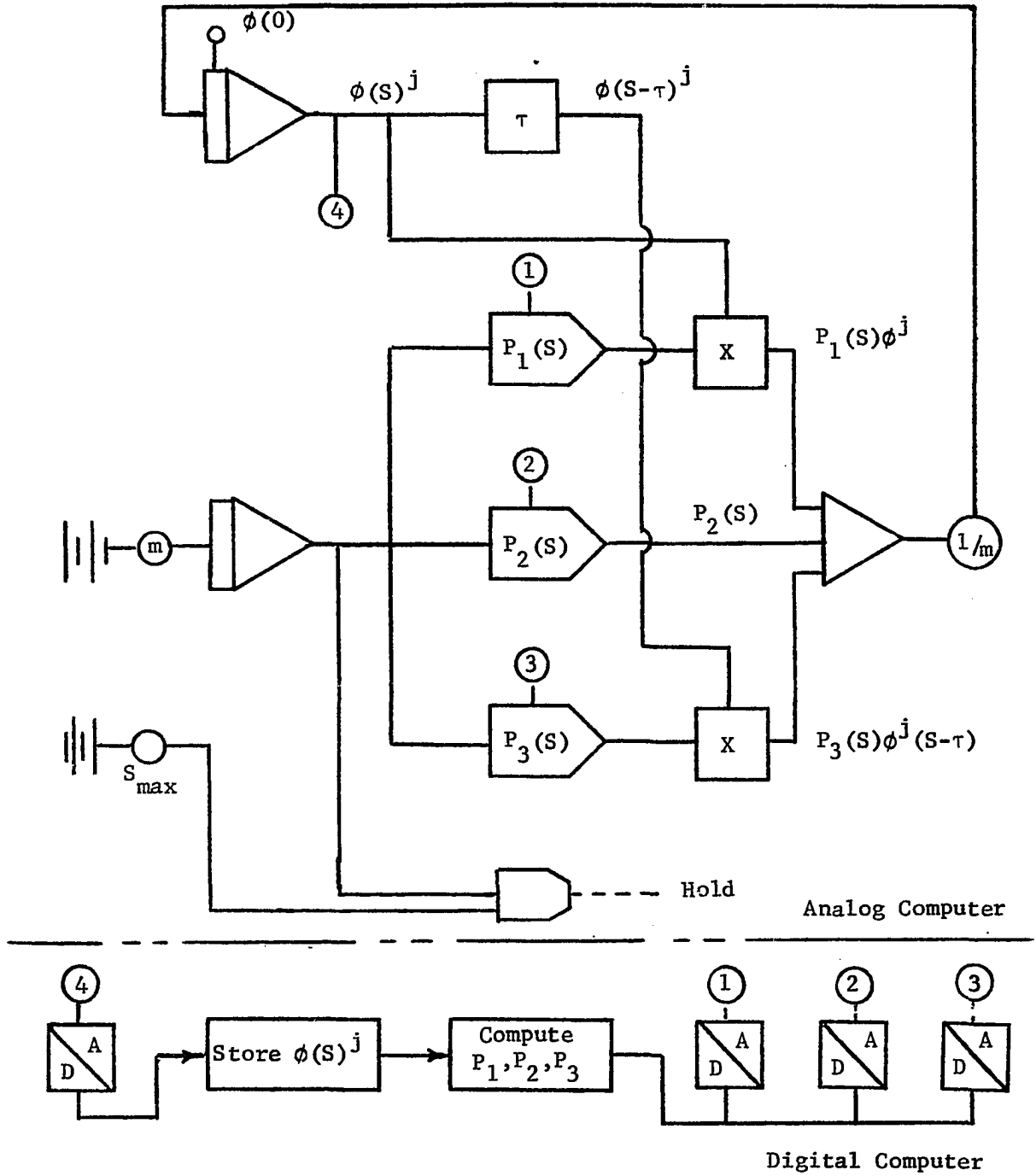


Figure 10. General analog diagram

their associated constant parameters are programmed on the digital computer. The flux values from the  $j-1$  sweep are sampled over the range of  $S$  and stored in the digital memory as they are computed. Between iteration sweeps, the digital computer determines the shape of the functions using this stored information. In one method of function generation, the digital outputs calculated breakpoints and slope values which are used to automatically or manually set up the function generators in preparation for the next sweep. Otherwise, function generation could be completely internal to the digital as described by Rubin (13).

The value of  $\phi_{i-1}^j$  is obtained by a time delay device which receives  $\phi_i^j$  as it is calculated and returns it to the calculations after a delay during which  $S$  has increased  $S_{\Delta\theta}$ , corresponding to the increments used in the calculation of functions  $P_1(S)$ ,  $P_2(S)$ , and  $P_3(S)$ .

After analog and digital programs for Equations 53, 55, and 56 have been developed, the general procedure of calculation of  $\phi(S)$  follows the sequence shown in Figure 11.

1. An initial distribution of flux,  $\phi^0$ , is stored in the digital memory. Initial values for the material cross sections and respective volume fractions, the region number for each point,  $k_1$  and  $k_2$  are also read.
2. The value of  $S$  at each sampling point and the material properties of each region are computed.
3. The functions  $P_1(S)$ ,  $P_2(S)$ , and  $P_3(S)$  are computed by the digital computer and applied to the function generators.

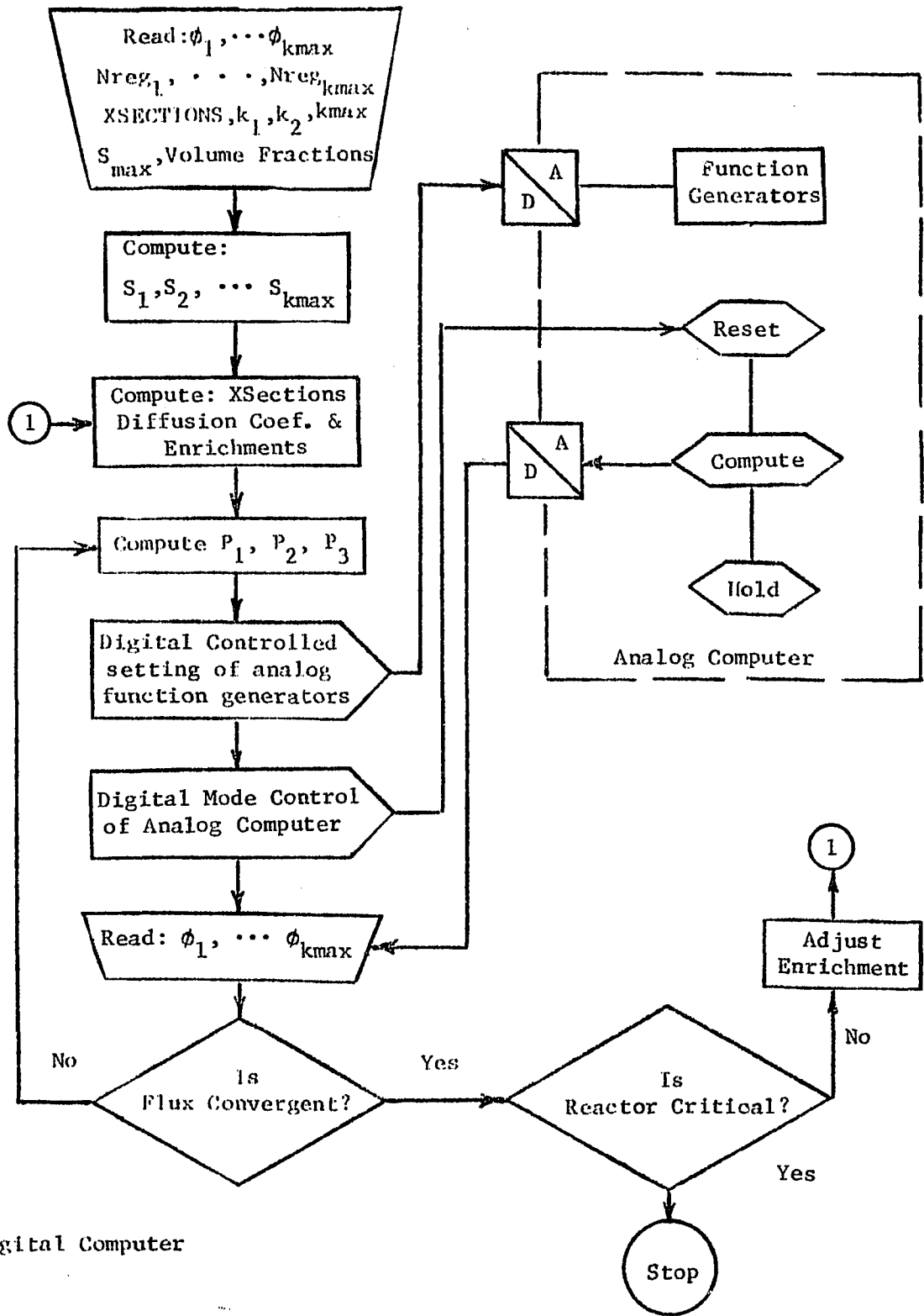


Figure 11. Flowchart for hybrid computation

4. The analog computer is "reset" and then put in "operate" mode, and the range of the parametric variable  $S$  is covered. During the sweep,  $j$ , through  $S$ , the function  $\phi(S)^j$  is computed by the analog, and  $k_{\max}$  samples are stored in the digital computer.
5. Once  $S = S_{\max}$  the analog is set in the "hold" mode, and the functions  $P_1(S)$ ,  $P_2(S)$ , and  $P_3(S)$  are recomputed.
6. Steps 3 and 4 are repeated until the digital has ascertained that  $\phi^{j-1}$  and  $\phi^j$  have converged.
7. The digital computer then tests for criticality and if necessary adjusts the enrichment of fissionable materials and repeats the entire program sequences beginning with the recalculation of nuclear parameters (step 3) until criticality is obtained.

Today's hybrid computers have digital computers with internal storage capacities of 32,000 bytes as well as tape and disk peripheral storage. Exclusive of array storage area, the digital program written for this study required 14,000 bytes of storage, thus leaving storage space for more than a thousand samples of the analog flux value if needed in step 4.

The analog computer serves chiefly as subroutine of the digital computer to determine the flux shape. In the next chapter a Gaussian reduction method operating on a set of difference equations has replaced the analog computer in this regard. Justification for using a hybrid computer to determine the two-dimensional flux shape would depend upon the need for the continuous distribution and the overall time dependent problem of which flux shape determination is but a part.

## V. DIGITAL COMPUTER SOLUTION OF THE TWO DIMENSIONAL DIFFUSION PROBLEM

A digital computer program using the Fortran IV language was written for the IBM-360/65 to check the validity and effectiveness of relating independent variables and to show that a common digital computer technique for one dimensional problems could be applied to related independent variables problems. The program considered the two dimensional diffusion equation applied to an infinite cylindrical reactor. In Section III the derivation of a set of finite difference equations was presented. The reactor was divided into N different areas along the path of the related independent variables, and the derivation of a difference equation for each area followed two dimensional procedures commonly used in formulation of two dimensional digital solutions. The difference equation for one area is expressed as

$$\alpha_1 \phi_{i+n} + \alpha \phi_{i+1} + \alpha_3 \phi_{i-n} + \delta \phi_{i-1} + [-\alpha_1 - \alpha - \alpha_3 - \delta + \sum_{k=1}^4 (v\Sigma_{f_k} - \Sigma_{a_k}) A_k] \phi_i = 0. \quad (57)$$

$\beta$  and  $\beta_S$  are defined

$$\beta = -\alpha_1 - \alpha - \alpha_3 - \delta - \sum_{k=1}^4 \Sigma_{a_k} A_k \quad (58)$$

and

$$\beta_S = \sum_{k=1}^4 v\Sigma_{f_k} A_k \quad (59)$$

so that for each region Equation 57 is simply written as

$$\alpha_1 \phi_{i+n} + \alpha \phi_{i+1} + \alpha_3 \phi_{i-n} + \delta \phi_{i-1} + \beta \phi_i + \beta_S \phi_i = 0. \quad (60)$$

When the set of difference equations describing all differential areas is written in matrix form, the resultant matrix is similar to a matrix

derived for a two dimensional problem when variables remain independent.

The matrices for the matrix equation

$$\bar{L}\bar{\phi} + \bar{S} = 0 \quad (61)$$

are shown in Figure 12. The chief difference between this  $\bar{L}$  matrix and the matrix arising in ordinary two dimensional problems is the continuation of non-tridiagonal terms into columns 1 and N. These terms are introduced by radial coupling during the first and last revolutions where the boundary conditions are imposed.

Dirichlet boundary conditions are easily considered for  $r = R$  by assigning an appropriate flux value to all points around the cylinder at  $r = R$ . Note that only the last point will lie on the spiral, all others will be on the circular outside boundary. In this formulation it is assumed that all flux values of  $r = R$  are equal to  $\phi_N$  so that during the last revolution of the spiral, if  $i + n > N$ ,  $\phi_{i+n} = \phi_N$ . This introduces the coefficients shown in column N of the L matrix. Neumann boundary conditions are imposed on the solution by assigning flux values to the outside physical boundary which meet the required slope conditions. The flux value at the center is unknown but  $\left. \frac{d\phi}{ds} \right|_{s=0}$  is approximated using the difference between two flux values calculated in the previous iteration. Also at the center where  $i - n < 0$ , the flux at the centerpoint is used for  $\phi_{i-n}$  in the approximation for the average derivative in Equation 29, so that  $\left( \frac{\partial \phi}{\partial r} \right) = \frac{\phi_i - \phi_{i-n}}{\Delta r} = \frac{\phi_i - \phi_1}{r_i - r_c}$ . This is the cause of the coefficient in the first column of the L matrix.

Adjustments for the change of shape of the differential area for the first and last revolutions of the spiral were accounted for in the calculation of all  $\alpha_i$ ,  $\beta_i$ ,  $\gamma_i$ ,  $\beta_{Si}$ , and  $\delta_i$  terms pertaining to the first and



last revolutions.

In order to retain the characteristic of a one dimensional solution, all products arising from elements of  $\bar{L}$  which were not tridiagonal were removed from  $\bar{L}$  and added to the source matrix, leaving  $\bar{L}$  in tridiagonal form. Equation 61 is then solved for  $\phi$  by the digital computer using Gaussian reduction.

The procedure followed in the solution of the Equation 61 is shown in Figure 13. The difference between the all digital and hybrid method is that Gaussian reduction has been replaced by the analog solution for  $\phi$ . The equations and order of procedure are basically the same and the values of  $\phi_{i+n}^{j-1}$  and  $\phi_{i-1}^{j-1}$  are used again in the solution of  $\phi_i^j$ . In this case, however,  $\phi_{i+n}^{j-1}$  has been rescaled to prevent the solution from diverging. The scaling factor,  $\rho$ , is defined by the vector product equation

$$(\rho^j)^2 = (\bar{\phi}^j, \bar{\phi}^j) \quad (62)$$

and is divided into  $\bar{\phi}_j$  before testing for convergence. Flux convergence was established by repeating inner iteration until

$$\left| \frac{\rho^{j-1}}{\rho^j} - 1 \right| < 0.00020.$$

The reactor was defined to be critical when

$$|\rho^j - 1| < 0.00001.$$

The flux shapes determined by this program are compared with a standard two dimensional program in the next section. A problem exactly similar in configuration and number of points was run to compare the related independent variables formulation with the two dimensional program using the alternating direction implicit method, it appears that the technique presented here is comparable in speed and

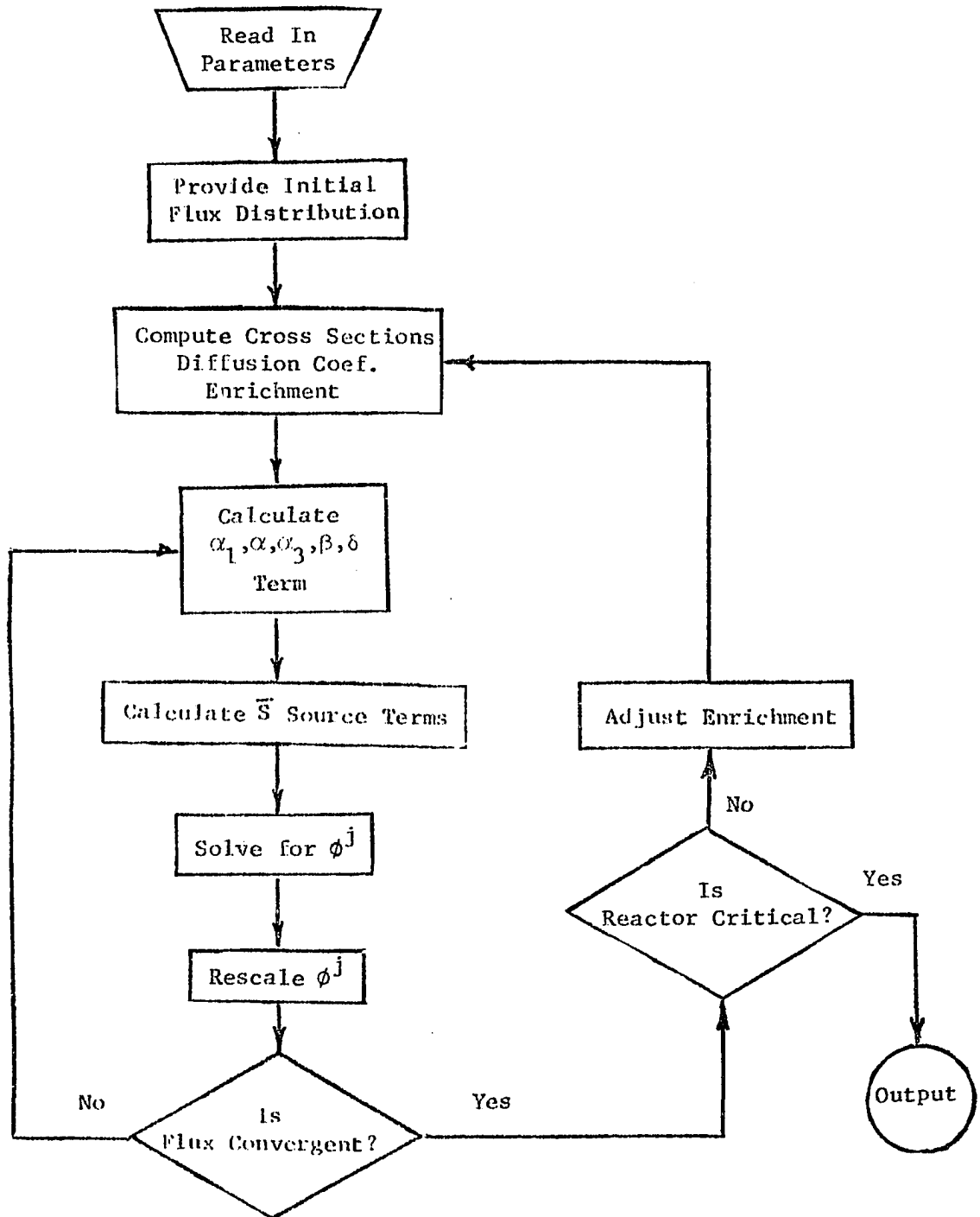


Figure 13. Digital computer flowchart

accuracy. A general comparison can be made by observing that a program using the related independent variables technique computed the flux shape shown in Figure 20 composed of 162 points in forty-four iterations, requiring 1.44 seconds to compile and 8.52 seconds to reach the convergence limits set above. The two dimensional program describing the same configuration with an equal number of points required forty-nine iterations to reach the same convergence limits. This second program required 1.36 seconds to compile and 22.14 seconds to complete the calculations of the flux shape shown also in Figure 20A. For the two examples cited, the total computer storage requirements were approximately equal.

## VI. RESULTS OF THE DIGITAL SOLUTION

As a preliminary study the related independent variables technique was applied to a homogeneous bare cylindrical reactor. Calculations involving ten revolutions of the spiral agreed with the theoretical solution as shown in Figure 14. Twenty revolutions gave the same agreement. The related independent variables solution shows no irregularities or discontinuities at either the center or outer boundary. Material buckling computed by the program checked the calculated geometric buckling for the 76.2 centimeters infinite cylinder to within 2%.

The digital computer program was then applied to various reactor geometries whose material configurations were described by  $r - \theta$  coordinates. The properties and geometries of three of the cases examined are shown in Figure 15. In all three cases the enrichment search was done by varying the U-235 composition in region II. For cases A and B, initially both regions were given identical materials and volume fractions. All regions were considered homogeneous. The volume fractions and cross sections as well as the materials and outer radius are those of the Argonaut Reactor (11). The angular velocity,  $k_2$ , and radial velocity,  $k_1$ , of the spiral were determined from considerations of the total number of points needed to accurately describe the geometry and yet minimize the amount of computer storage required.

Figures 16 through 20 show the one-group steady-state flux distributions for the three configurations. The distributions determined by the digital computer program described in the last chapter are compared with a two dimensional digital code for each case.

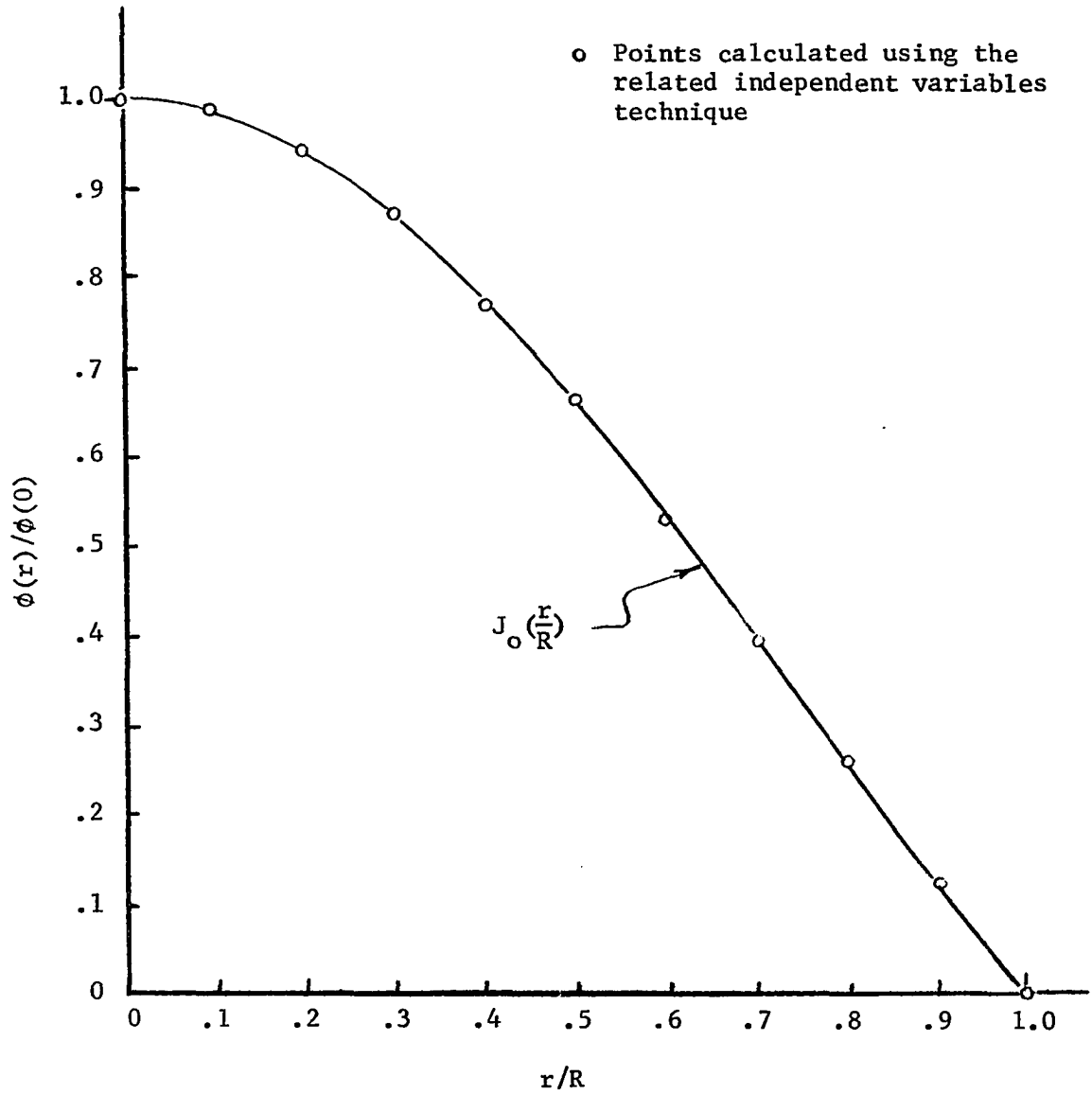
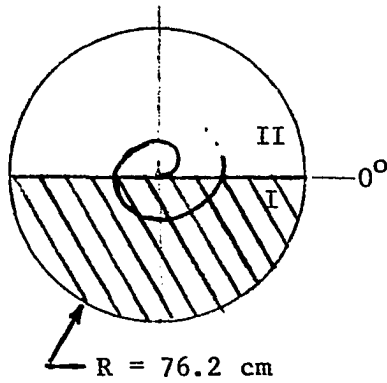
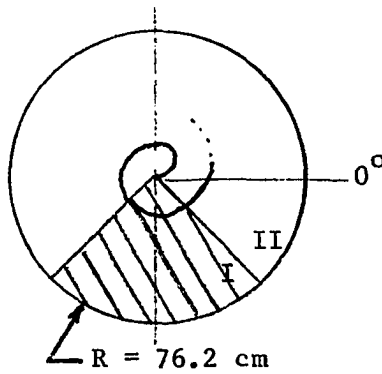


Figure 14. Comparison of theoretical and related variables solution to a bare homogeneous reactor



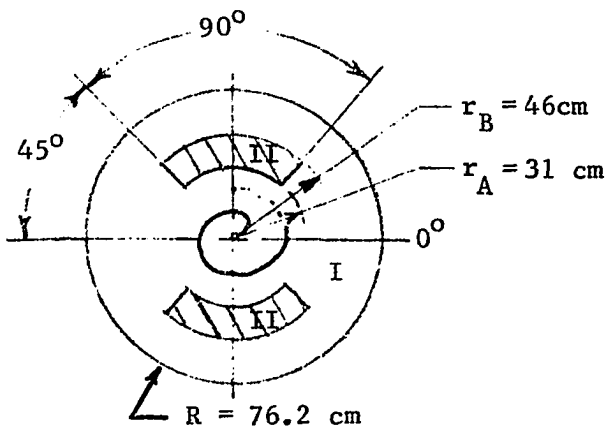
Case A

Materials	Volume Fractions
U-235	0.00045
U-238	0.00135
H <sub>2</sub> O	0.52600
Graphite	0.25320
Aluminum	0.21900



Case B

Materials	Volume Fractions
U-235	0.00045
U-238	0.00135
H <sub>2</sub> O	0.52600
Graphite	0.25320
Aluminum	0.21900



Case C  
Argonaut Geometry

Region Number	Materials	Volume Fractions
I	Graphite	1.00000
II	U-235	0.00040
	U-238	0.00160
	H <sub>2</sub> O	0.52600
	Graphite	0.25300
	Aluminum	0.21900

Figure 15. Three cases studied using the digital program

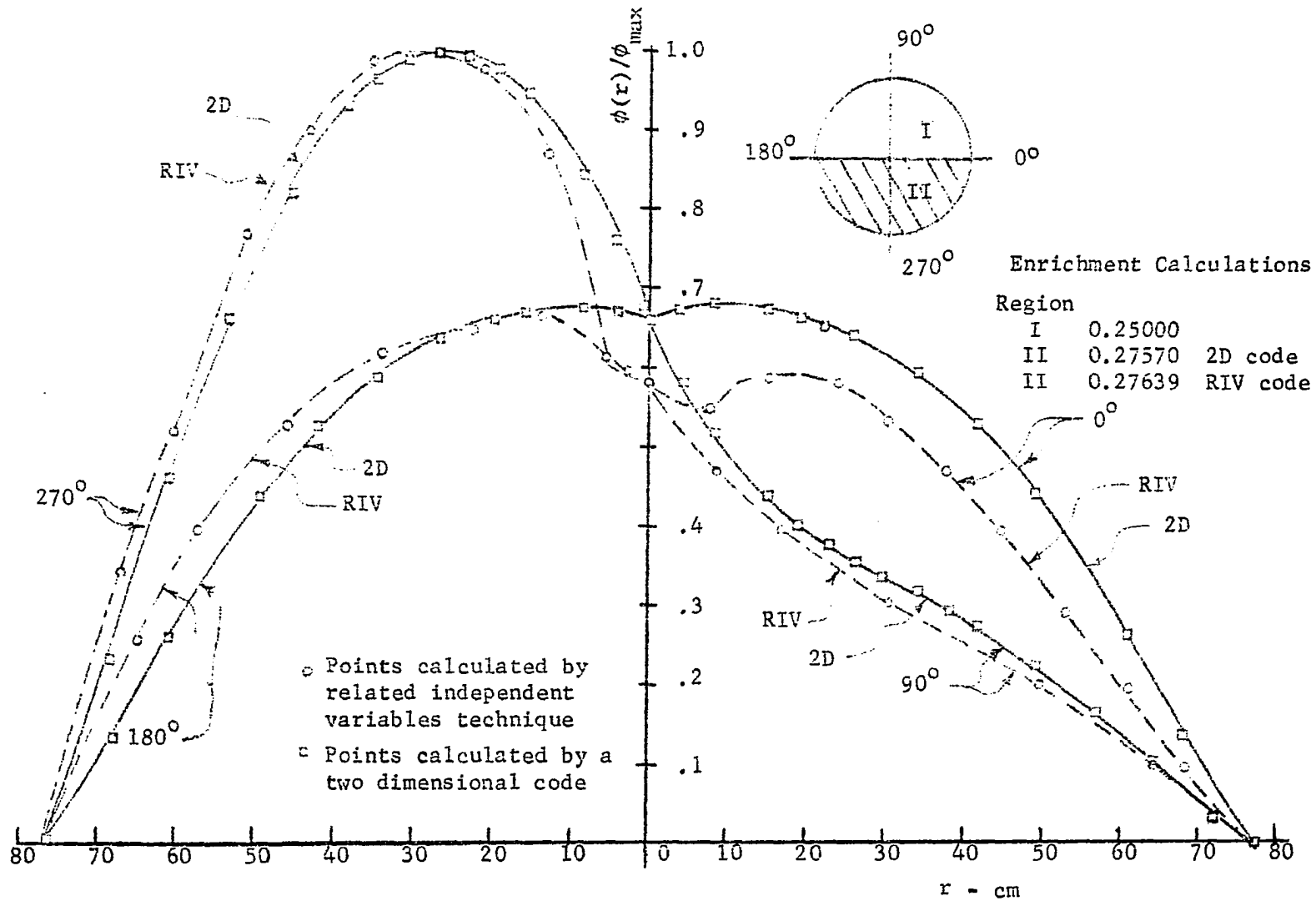


Figure 16. Flux profiles for Case A using 160 space points in ten spiral revolutions of the related independent variables  $r$  and  $\theta$

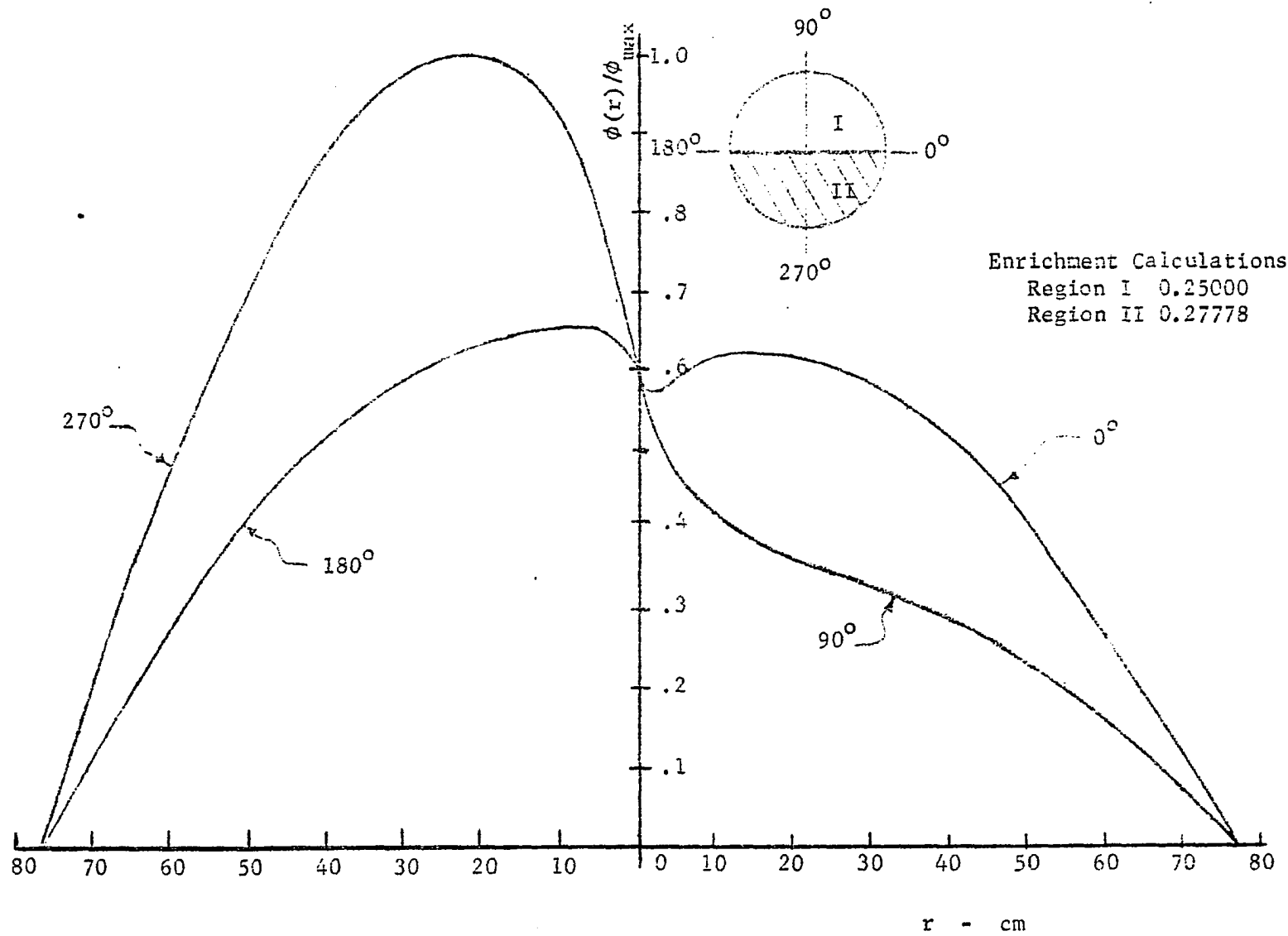


Figure 17. Flux profiles for Case A using 320 space points in twenty spiral revolutions of the related independent variables  $r$  and  $\theta$

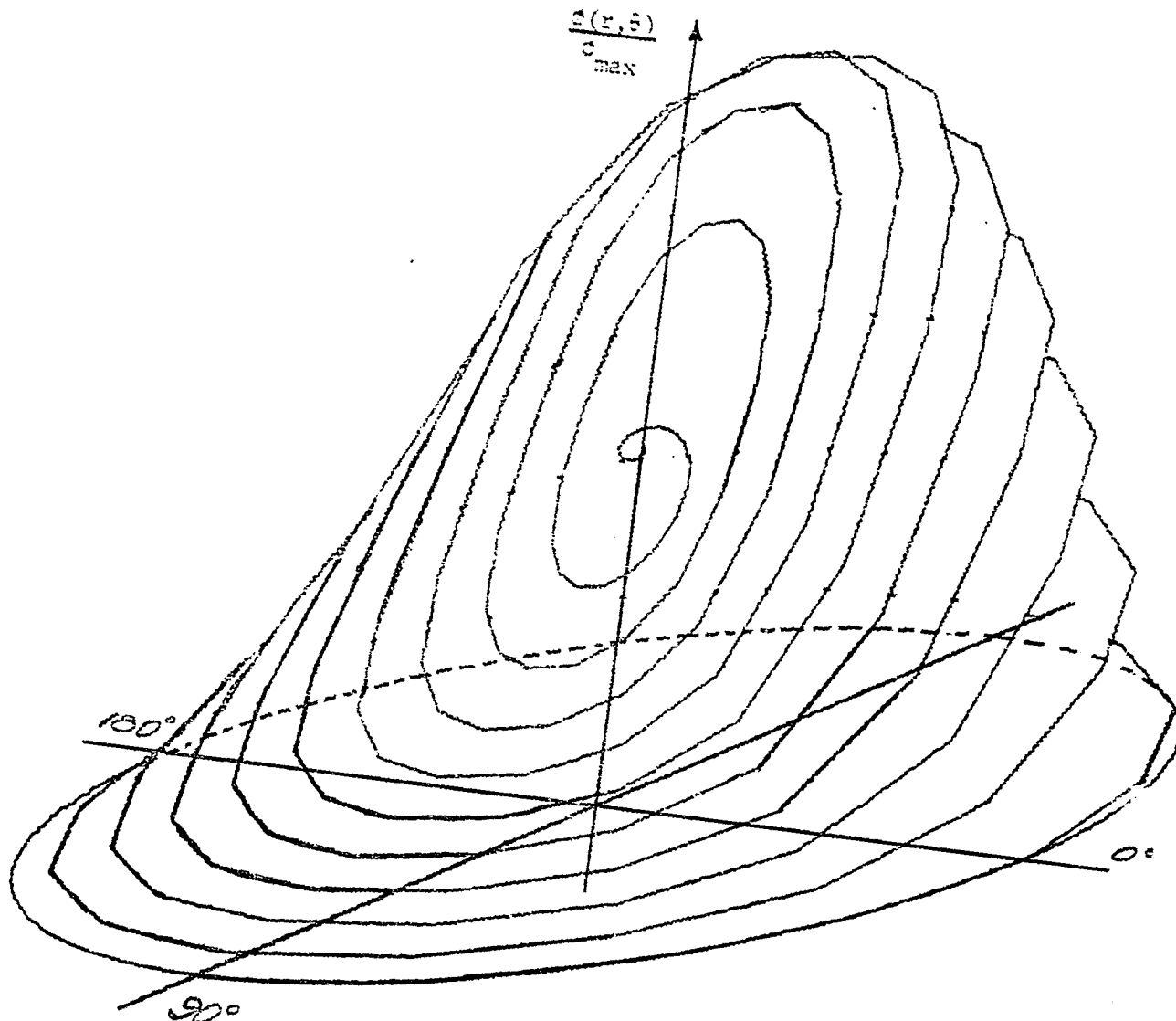


Figure 18. A spiral representation of the three dimensional flux shape for Case A shown as flux profiles in Figure 17

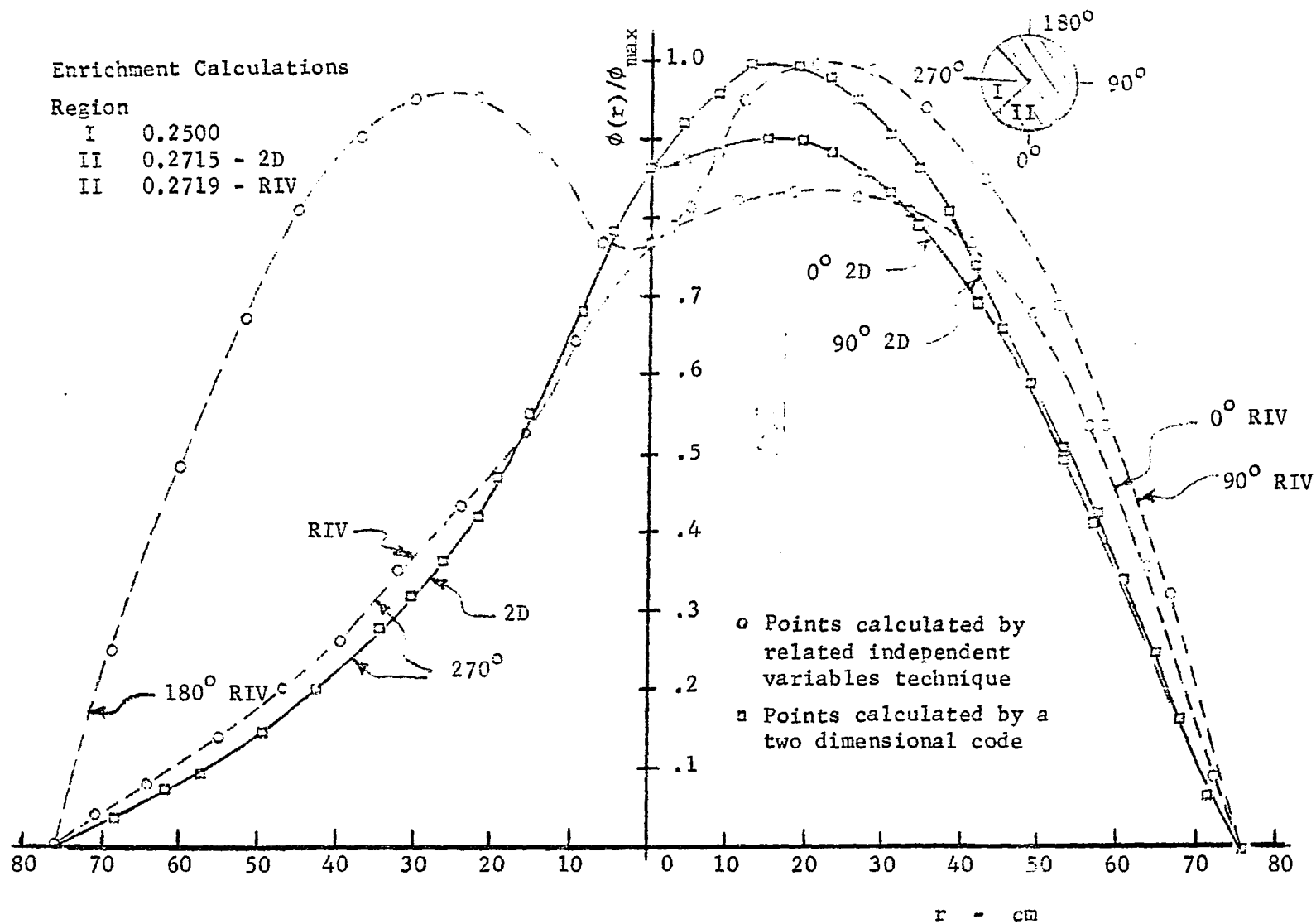


Figure 19. Flux profiles for Case B using 160 space points in ten spiral revolutions of the related independent variables  $r$  and  $\theta$

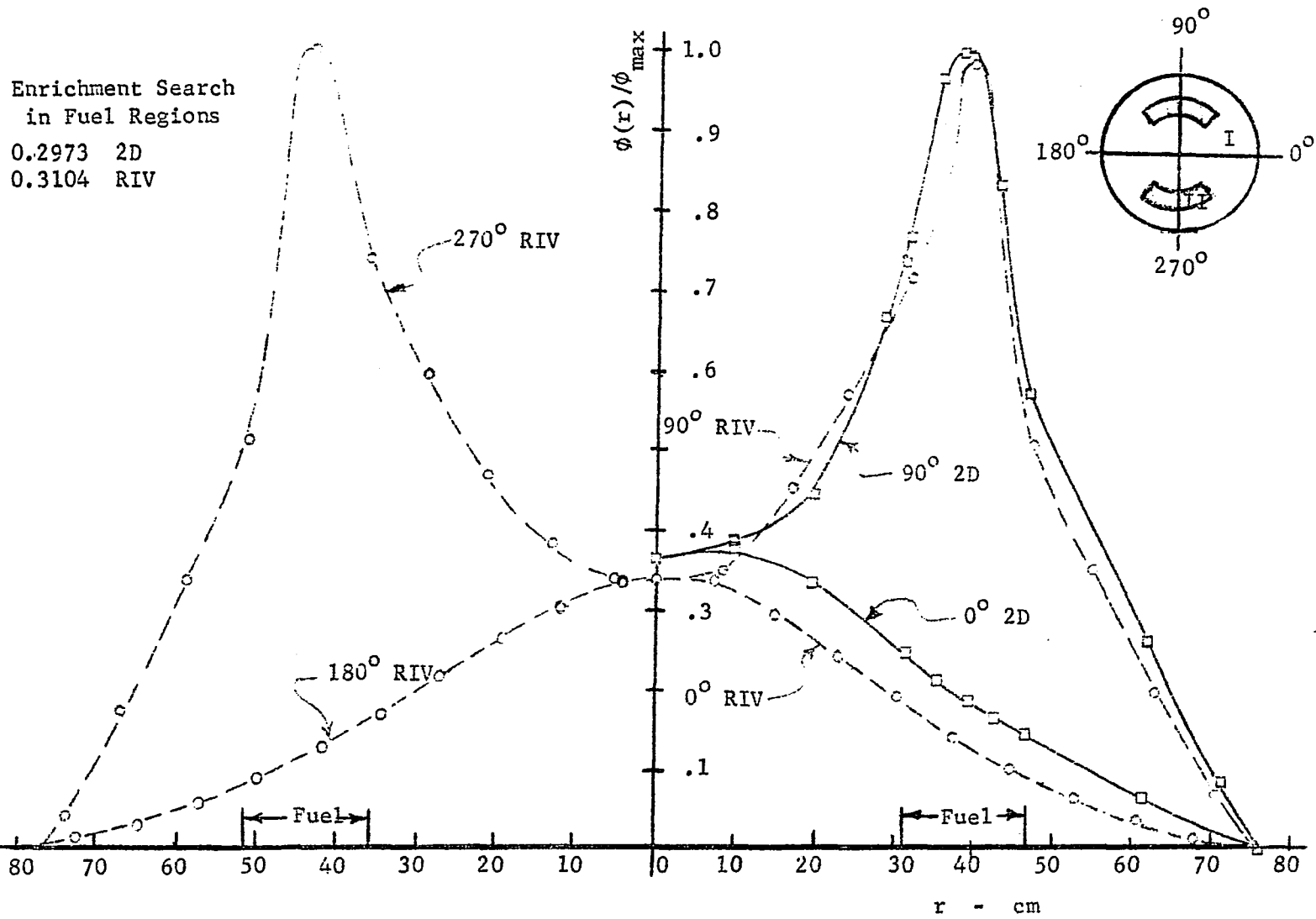


Figure 20. Flux profiles for Case C using 160 space points in ten spiral revolutions of the related independent variables  $r$  and  $\theta$

Enrichment Search  
in Fuel Regions  
.30555 - 2D

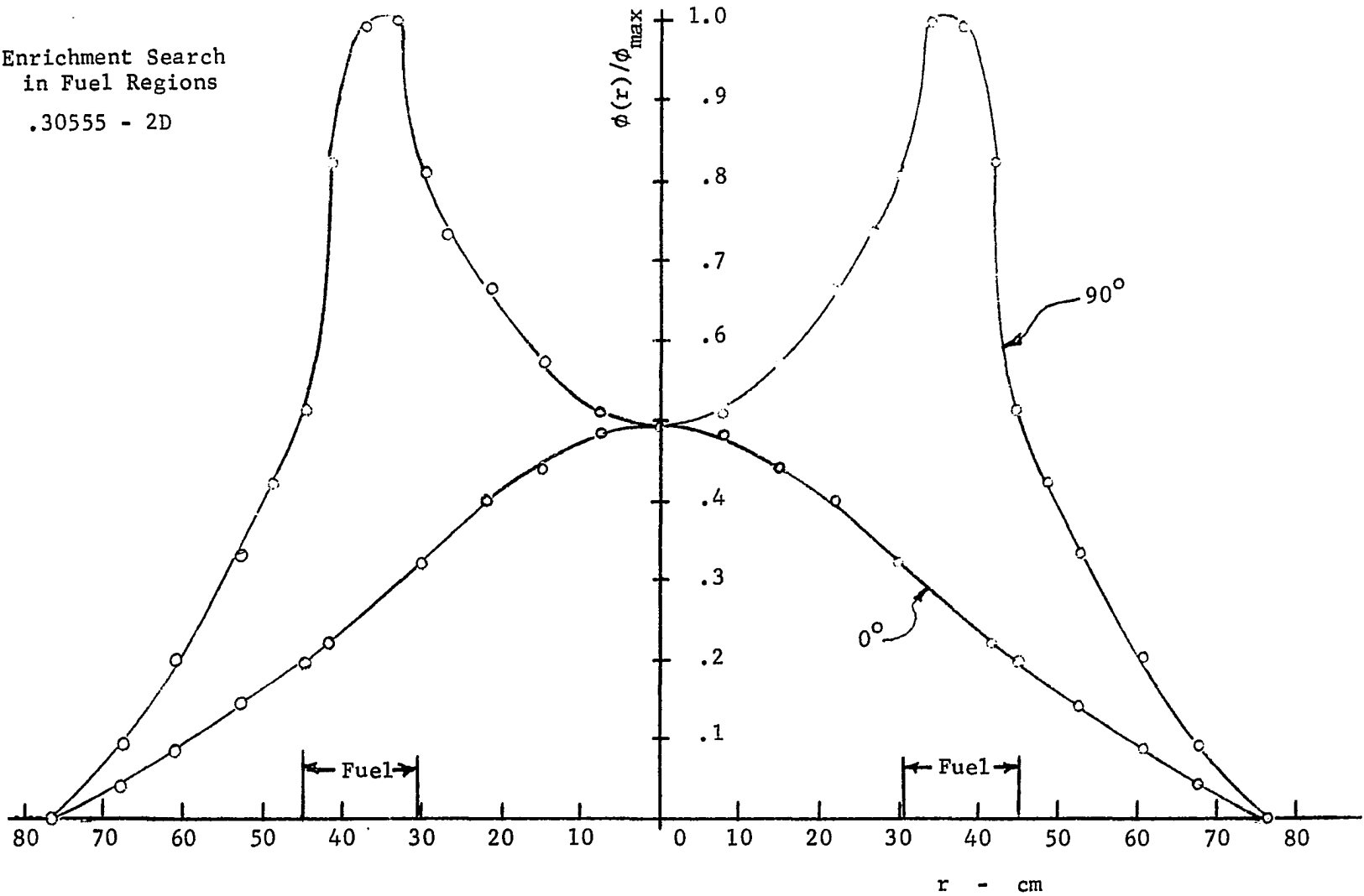


Figure 20A. Flux profile for Argonaut geometry without skewed fuel regions (determined by two dimensional program)

The flux profiles of cases A and B show the discontinuity that arises at the center of the reactor when a flux gradient exists at the center of the reactor. This discontinuity is not seen in the homogeneous reactor, nor is it found to exist in the Argonaut geometry (Figure 20) where the center region is homogeneous and flux tilting has not been considered.

Attempts to remove the flux depression in the center were not successful. The effect of increasing the angular velocity and thus tightening the spiral is shown in Figure 17 for case A. Increasing the radius of the incremental circle at the center beyond  $S = 0.001$  was not effective in reducing the flux depression. Besides the approximations at the center previously described in Section III, several other less rigorous approximations were attempted without success. These included the replacement of the incremental circle around  $r = 0$  with a small spiral; linear approximations at the center of one or all of the coefficients  $\alpha_1$ ,  $\alpha$ ,  $\alpha_3$ ,  $\beta$ , and  $\delta$ ; and the specification of the slope of  $\frac{d\phi}{dS}\Big|_{S=0}$ . At first appearances the attempt to specify  $\frac{d\phi}{dS}\Big|_{S=0}$  seemed to be important. However, for cases A and B, it was found that irrespective of the value of  $\frac{d\phi}{dS}\Big|_{S=0}$  and the initial direction of the spiral ( $\theta = 0$ ) with respect to the location of the asymmetric subcritical region, symmetry of the flux profile about  $r = 0$  for  $\theta = 90^\circ$  was not found in regions near the center but was realized at values of  $r$  greater than  $0.4R$ .

In view of the variety of center region approximations attempted without success, it is concluded that the related independent variables technique cannot be applied to configurations involving a gradient in the flux profile at  $r = 0$ . The approximations presented in Section III for the first revolution of the spiral appear at present to be adequate for

describing configurations where the effect of a perturbation does not strongly affect the flux profile at the center of the reactor.

When considering geometries with material regions located at a radial distance from the center, it is necessary to approximate the interfaces marked by lines of constant  $r$  with skewed lines of the spiral. In the solution of the flux shape of the Argonaut reactor geometry with only ten revolutions, this approximation required that material interfaces of the internal reflector vary from the true radius of 31.43 centimeters to 33.81 centimeters as the spiral traced one-fourth of a revolution. Likewise the outer edge of the fuel region was also moved from the true 46.20 centimeters to 48.58 centimeters so that the boundary would conform to the contour of the spiral. The effect of this fuel movement on the flux shape is shown in Figure 20A. Increasing  $k_2$  relative to  $k_1$  would reduce this radial shifting and improve the approximation.

## VII. SUMMARY AND CONCLUSIONS

In this study a technique has been proposed and developed for introducing parametric variables into the Laplacian operator as a means of reducing the number of independent variables required in the solution of the dependent variable. The results of a digital code based on the related independent variables technique have shown that this approach compares favorably with neutron flux shapes determined by another method of two dimensional digital computer computations as long as a flux gradient does not occur at  $r = 0$ . The extension of this technique to multi-group and reactor transient calculations based upon conventional coordinate systems would be accomplished using the same procedures followed in extending steady state one group calculation methods.

The related independent variables technique has been proposed as a means of expanding continuous space discrete time hybrid computer solutions to multidimensional geometries. This technique appears to be applicable to digital computer calculations also. A significant savings in running times were observed between an ordinary two dimensional program and a program based on the related independent variables technique.

In this study, only the Laplacian operator has been considered. Application of this technique to other mathematical expressions may produce similar reductions in the number of independent variables and such reductions may be useful in both hybrid and digital computations.

## VIII. SUGGESTIONS FOR FURTHER STUDY

The results of this study indicate that for certain types of reactor configurations there is merit in the technique of relating the independent variables. The next logical step in developing this technique in reactor applications is to consider more intricate geometries and to apply the technique to multi-group and reactor transient problems. It would also be interesting to extend the related independent variables technique to boundary value problems arising in other areas of engineering and to examine the possibilities of eliminating the limitations encountered in the nuclear application. These further studies would be of greater significance if implemented using a hybrid computer.

The development in this study has basically followed the methods used in the formulation of a set of difference equations for the description of a two dimensional problem. Another approach to a similar two dimensional study would be to use finite difference approximations for the partial derivatives in the Laplacian operator without first integrating over the differential area. In such an approach, in addition to the parametric equations in  $S$  for the variables  $r$  and  $\theta$  used here, the expressions

$$\frac{\partial \phi}{\partial S} = k_1 \frac{\partial \phi}{\partial r} + k_2 \frac{\partial \phi}{\partial \theta}$$

and

$$\frac{\partial^2 \phi}{\partial S^2} = k_1^2 \frac{\partial^2 \phi}{\partial r^2} + 2k_1 k_2 \frac{\partial}{\partial r} \frac{\partial \phi}{\partial \theta} + k_2^2 \frac{\partial^2 \phi}{\partial \theta^2}$$

would be used to eliminate  $r$  and  $\theta$  from the Laplacian. It has been pointed out by Vichnevetsky (16) that for ordinary coordinate systems the finite difference approximations in the radial direction have the undesirable

property of increasing the number of differential equations that must be solved and the number of boundary conditions that must be considered. In this study, by expressing the independent variables in terms of one continuous parametric variable, these additional differential equations have been eliminated. The substitutions suggested above would be another approach to applying the related independent variables technique to a hybrid computer.

## IX. LITERATURE CITED

1. Bona, C. Analog simulation of PWR plant with space-time core equations. European Atomic Energy Community EUR-3112.i Rome, Italy. 1966.
2. Caliguiri, G. P., Claes, W., d'Hoop, H., and Vichnevetsky, R. Research on three dimensional simulation of nuclear reactors. Proceedings of the third International AICA Meeting, 1961. European Academic Press, Brussels, Belgium. 1962. Original not available; cited in Vichnevetsky, R. Analog/hybrid solution of partial differential equations in the nuclear industry. Simulation 11:269-281. 1968.
3. Calza-Bini, A. Proceedings of the 5th International AICA Congress, 1967, Brussels, Belgium. European Academic Press. 1967. Original not available; cited in Vichnevetsky, R. Analog/hybrid solution of partial differential equations in the nuclear industry. Simulation 11:269-281. 1968.
4. Carstairs, R. L. and Taylor, R. W. The occurrence and control of spatial instabilities in large reactors. G.E.C. Atomic Energy Review. Vol. 2, No. 2. September 1959. Original not available; cited in Vichnevetsky, R. Analog/hybrid solution of partial differential equations in the nuclear industry. Simulation 11:269-281. 1968.
5. Carstairs, R. L. and Taylor, R. W. Reactor radial spatial behavior. Nuclear Power. June 1960. Original not available; cited in Vichnevetsky, R. Analog/hybrid solution of partial differential equations in the nuclear industry. Simulation 11:269-281. 1968.
6. d'Hoop, H. La simulation dynamique a trois dimensions des grands reacteur nucleares. Centre European le Traitement Les Informations Scientifiques:18. Ispra, Italy, CETIS. 1963.
7. Godts, J. E. Analog analysis of transient neutron flux by discontinuous synthesis. Unpublished Ph.D. thesis. Pittsburgh, Pa., Library, Carnegie Institute of Technology. 1965.
8. Howe, R. M. and Haneman, V. S. The solution of partial differential equations by difference methods using the electronic differential analyzer. Institute of Radio Engineers Proceedings 41:1497-1508. 1953.
9. Karplus, Walter J. Analog simulation. New York, N.Y., McGraw-Hill Book Co., Inc. 1958.
10. Karplus, Walter J. and Soroka, Walter W. Analog methods. 2nd ed. New York, N.Y., McGraw-Hill Book Co., Inc. 1959.

11. Kelber, Charles N. The theoretical physics of the Argonaut reactor. U.S. Atomic Energy Commission Report ANL 5710 [Argonne National Laboratory, Lemont, Illinois]. 1957.
12. MacKay, Donald M. and Fisher, Michael E. Analogue computing at ultra-high speed. New York, N.Y., John Wiley and Sons, Inc. 1962.
13. Rubin, Arthur I. Hybrid techniques for generation of arbitrary functions. Simulation 7:293-305. 1966.
14. Sangren, Ward C. Digital computers and nuclear reactor calculations. New York, N.Y., John Wiley and Sons, Inc. 1960.
15. Tomovic, Rajko and Karplus, Walter J. High speed analog computers. New York, N.Y., John Wiley and Sons, Inc. c1962.
16. Vichnevetsky, R. Analog/hybrid solution of partial differential equations in the nuclear industry. Simulation 11:269-281. 1968.
17. Vichnevetsky, R. Application of hybrid computers to the integration of partial differential equations of the first and second order. Proceedings of IFIP Congress, 1968, Edinburgh, Scotland. 1968. Original not available; cited in Vichnevetsky, R. Analog/hybrid solution of partial differential equations in the nuclear industry. Simulation 11:269-281. 1968.
18. Witsenhausen, H. S. Hybrid solution of initial value problems for partial differential equations. Massachusetts Institute of Technology. Electronic Systems Laboratory Memorandum No. 8. 1964. Original not available; cited in Vichnevetsky, R. Analog/hybrid solution of partial differential equations in the nuclear industry. Simulation 11:269-281. 1968.
19. Wylie, G. R., Jr. Advanced engineering mathematics. 2nd ed. New York, N.Y., McGraw-Hill Book Co., Inc. 1960.

X. ACKNOWLEDGMENTS

A thesis is not the product of one individual but is really a concert of talents, facilities, interests, and inspirations from several sources. The author wishes to thank the following for their various contributions.

Dr. Alfred F. Rohach

Dr. Glenn Murphy

Dr. Richard E. Turley

Iowa State University

Fellow Students

Mr. and Mrs. Leonard J. Jaworski

and

Paula, my wife

XI. APPENDIX A - THE CONTINUOUS SPACE, DISCRETE TIME METHOD  
 APPLIED TO PARABOLIC DIFFUSION EQUATIONS

In this appendix the hybrid computer CSDT method of solving the parabolic diffusion equation is described. For this illustration, neutron flux kinetic equations are given in the simplified form:

$$l \frac{\partial \phi(z,t)}{\partial t} = M^2 \frac{\partial^2 \phi(z,t)}{\partial z^2} + (K - 1)\phi(z,t) \quad (\text{A-1})$$

where:

$l$  = the neutron life time

$M^2$  = the migration area

$\phi$  = the neutron flux

$K$  = the effective multiplication factor.

By assuming fixed time intervals,  $t_i = i\Delta t$  and  $\phi_i \approx \phi_{i+1}$ , Equation A-1 is approximated by a sequence of ordinary differential equations

$$l \frac{\phi_{i+1} - \phi_i}{\Delta t} = \theta \left[ M^2 \frac{d^2}{dz^2} + K - 1 \right] \phi_{i+1} + (1 - \theta) \left[ M^2 \frac{d^2}{dz^2} + K - 1 \right] \phi_i \quad (\text{A-2})$$

where  $\theta$  is an arbitrary scalar  $< 1$ . Equation A-2 can be written as

$$\frac{d^2 \phi_{i+1}}{dz^2} - \left[ \frac{l}{M^2 \theta \Delta t} - \frac{K - 1}{M} \right] \phi_{i+1} = - \frac{l}{M^2 \theta \Delta t} S_i \quad (\text{A-3})$$

where

$$S_i = \phi_i + (1 - \theta) \frac{\Delta t}{l} \left( M^2 \frac{d^2}{dz^2} + K - 1 \right) \phi_i. \quad (\text{A-4})$$

$S_{i+1}$  is derived by recursion relationship from  $S_i$ . From Equation A-4,

$$S_{i+1} = \phi_{i+1} + (1 - \theta) \frac{\Delta t}{l} \left( M^2 \frac{d^2}{dz^2} + K - 1 \right) \phi_{i+1}$$

$$S_{i+1} = S_i + \frac{1}{\theta} (\phi_{i+1} - S_i) \quad (\text{A-5})$$

where the initial value of  $S_0$  is  $\phi(z,0)$ .  $S_{i+1}$  is computed by the digital while outputting  $S_i$ . The block diagram of hybrid computer function storage and playback is shown in Figure 21. Four methods are available for solving Equations A-3, A-4, and A-5. They are:

1. the shooting method
2. the superposition method, Calza-Bini (3)
3. Green's function method, Witsenhausen (18)
4. the Decomposition method, Vichnevetsky (17).

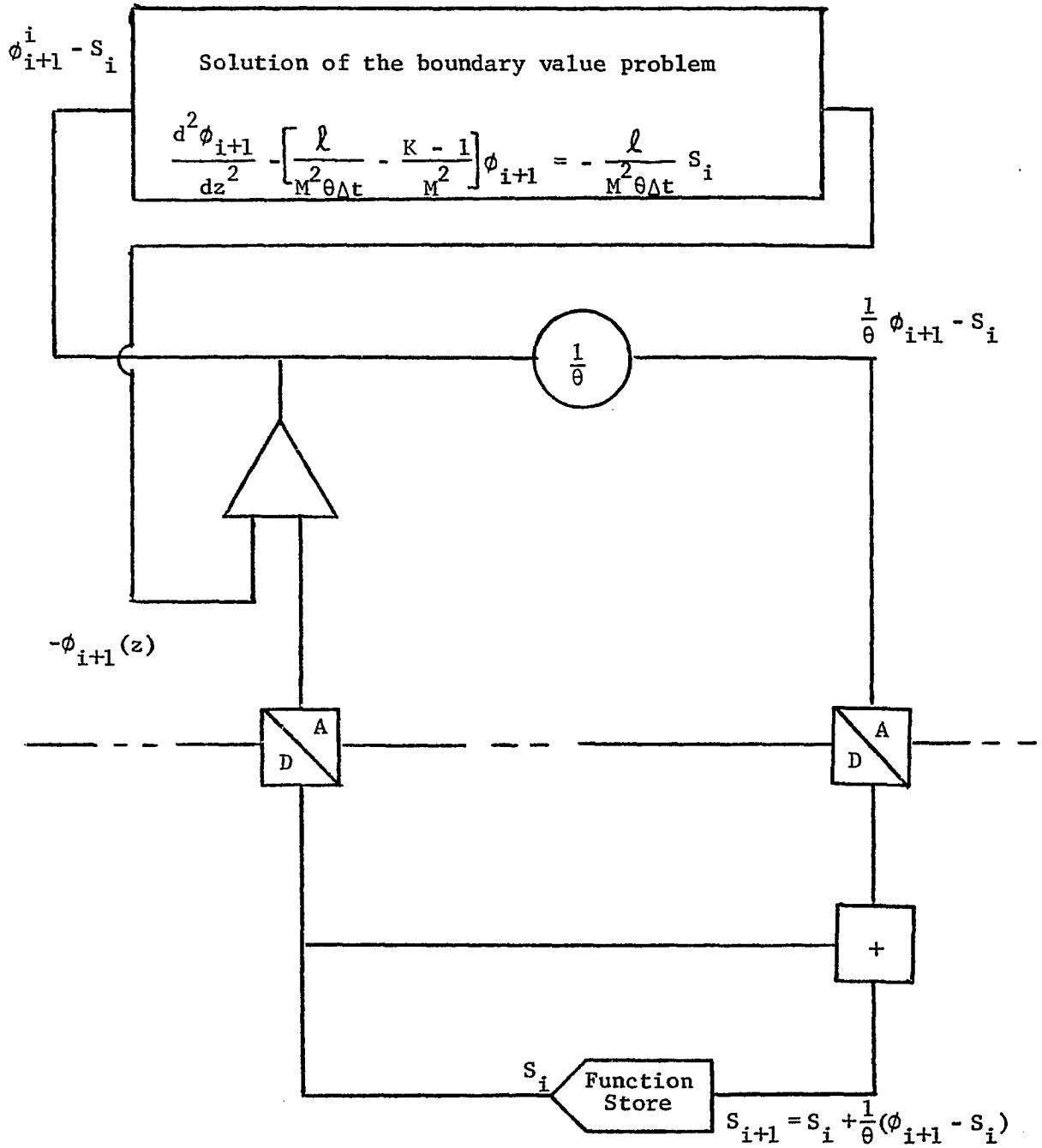


Figure 21. Hybrid circuit diagram for CSDT solution of diffusion equation

XII. APPENDIX B - THE PARALLEL MODAL METHOD APPLIED  
TO THE PARABOLIC DIFFUSION EQUATION

In this appendix, the procedures for applying the parallel modal method to a cylindrical nuclear reactor will be outlined. A simplified form of the neutron kinetics equation is used.

$$\lambda \frac{\partial}{\partial t} \phi(r, \theta, z, t) = M^2 \nabla^2 \phi(r, \theta, z, t) + (K - 1) \phi(r, \theta, z, t) + S \quad (\text{B-1})$$

where  $S$  is a source term and the other notation used is explained in Appendix A.

Let

$$\phi(r, \theta, z, t) \approx \sum_{i=1}^N \rho_i(t) f_i(r, \theta, z) \quad (\text{B-2})$$

where  $f_i$  are the eigenfunctions of the Helmholtz equation

$$\nabla^2 f_i(r, \theta, z) = \lambda_i f_i(r, \theta, z) \quad (\text{B-3})$$

and also satisfy the boundary conditions of  $\phi$ .

The eigenfunctions have the orthogonality property

$$\int_{\text{Volume}} f_i f_j \, d(\text{Volume}) = 0 \quad i \neq j. \quad (\text{B-4})$$

When the  $\phi(r, \theta, z, t)$  expressed in Equation B-2 is substituted into Equation B-1 and the resulting equation is integrated over the volume of the reactor, the orthogonality property is used to obtain the following set of  $N$  ordinary differential equations

$$\lambda \frac{d \rho_i(t)}{dt} = (M^2 \lambda_i + K - 1) \rho_i(t) + \int_{\text{Volume}} S f_i \, d(\text{Volume}). \quad (\text{B-5})$$

These equations are solved simultaneously on an analog computer to obtain the time dependent coefficients  $\rho_i(t)$ .

In heterogeneous reactor problems where parameters are space and time dependent, solution for several multidimensional modes and representation of parameters in Equation B-5 seriously complicate the overall solution.

XIII. APPENDIX C - THE MIXED MODAL-SERIAL METHOD APPLIED  
TO THE PARABOLIC DIFFUSION EQUATION

This method is used for application of CSDT technique to problems involving more than one space variable. The modal technique, outlined in Appendix B, is used to eliminate partial derivatives of noncontinuous space dimensions.

The parabolic diffusion equation applied to a cylindrical reactor is described by an  $r - z$  coordinate system

$$\ell \frac{\partial \phi(r,z,t)}{\partial t} = \left[ M^2 \left( \frac{\partial^2}{\partial z^2} + \frac{\partial^2}{\partial r^2} + \frac{1}{r} \frac{\partial}{\partial r} \right) + K - 1 \right] \phi(r,z,t) \quad (C-1)$$

When considering the  $z$  dimensions as continuous, the radial flux dependence is considered in terms of radial modes.  $\phi$  is expanded by the modal approximation

$$\phi(r,z,t) = \sum_{m=1}^N \rho_m(z,t) f_{mr}(r) \quad (C-2)$$

where  $f_{mr}$  are the eigenmodes of the equation

$$\frac{\partial^2}{\partial r^2} + \frac{1}{r} \frac{\partial}{\partial r} f_{mr} = \lambda_{mr} f_{mr} \quad (C-3)$$

When the Equation C-3 is substituted into Equation C-1, the result is

$$\ell \frac{\partial \rho_m(z,t)}{\partial t} = \left[ M^2 \left( \frac{\partial^2}{\partial z^2} + \lambda_{mr} \right) + K - 1 \right] \rho_m(z,t) \quad (C-4)$$

$m = 1, \dots, N$

Use of the difference approximation for the time derivative then yields

$$\ell \left( \frac{\rho_{m,i+1} - \rho_{m,i}}{\Delta t_i} \right) = \left[ M^2 \left( \frac{d^2}{dz^2} + \lambda_{mr} \right) + K - 1 \right] \rho_{m,i+1} \quad (C-5)$$

which is a set of  $N$  ordinary differential equations continuous in the  $z$  coordinate. This set of equations is solved by the CSDT procedure illustrated in Appendix A.